Review

Bioinspired Stimuli-responsive Materials for Soft Actuators

Zhongbao Wang , Yixin Chen , Yuan Ma * , Jing Wang *

Posted Date: 29 January 2024

doi: 10.20944/preprints202401.2039.v1

Keywords: Bioinspired actuators; soft robots; stimuli-responsive materials; smart materials

Review

Bioinspired Stimuli-Responsive Materials for Soft Actuators

Zhongbao Wang [1], Yixin Chen [1], Yuan Ma [2,*] and Jing Wang [1,*]

[1] State Key Laboratory of Mechanical System and Vibration, School of Mechanical Engineering, Shanghai Jiao Tong University, Shanghai, China.

[2] Research Institute for Intelligent Wearable Systems, Department of Mechanical Engineering, The Hong Kong Polytechnic University, Hong Kong, China.

* Correspondence: juw6@sjtu.edu.cn

Abstract: Biomimetic stimuli-responsive materials can respond to various external stimuli in the form of structural or morphological transformations by actively or passively converting input energy into mechanical energy. They are the core element of soft actuators for typical smart devices like soft robots, artificial muscles, intelligent sensors and nanogenerators. While significant progresses have been made in bioinspired stimuli-responsive materials, they have not yet achieved the remarkable properties in biological systems. In this review, we will discuss recent advances in biomimetic stimuli-responsive materials that are instrumental for soft actuators. Different stimuli-responsive principles for soft actuators are firstly discussed, including fluidic, electrical, thermal, magnetic, light and chemical stimuli. We further summarize the state-of-the-art stimuli-responsive materials for soft actuators and explore the advantages and disadvantages of using electroactive polymers, magnetic soft composites, hydrogels, liquid crystal elastomers, shape memory alloys and chemical-responsive materials. Finally, we provide a critical outlook on the field of stimuli-responsive soft actuators, and emphasize the challenges in the process of their implementation to various industries.

Keywords: Bioinspired actuators; soft robots; stimuli-responsive materials; smart materials

1. Introduction

Inspired by deformable, adaptive and reconfigurable environmental-responsive biomaterial systems in nature, artificial stimuli-responsive materials based on external physical and/or chemical stimuli have been developed for a variety of emerging industrial and household applications [1–4]. Compared to the conventional rigid actuators, soft actuators based on stimuli-responsive materials are composed of soft matters, that is, polymers, elastomers or flexible composites. Their Young's modulus is typically lower than 1 GPa, which is only 1/200 of the Young's modulus of the rigid actuator's [5–7]. The excellent flexibility and adaptability of stimuli-responsive materials make soft actuators an ideal and critical element to be adopted in soft robots [8–10], artificial muscles [11–15], wearable haptics [16–20], and exoskeletons [21–25].

While great progresses have been made in soft actuators, the implementation for real-world applications remains a challenge because of the limitations in activating conditions and some property flaws in current stimuli-responsive materials [26–28]. Some soft actuators still retain complex circuits or pipelines to connect external power supplies for effective actuation. In this case, with the need in implementing "tailless" design, these actuators have low degrees of freedom in motion as well as poor flexibility and adaptability that limit their applications in complex environments or narrow spaces. For example, pneumatic actuators require air pumps and control valves, which increases the volume and weight of the system [29–31]. Moreover, dielectric elastomer actuators often rely on high driving voltages of hundred-volts or kilo-volts for large deformations, which could bring serious safety concerns [32–35].

Practical applications of stimuli-responsive materials in soft actuators are also hindered by material properties in terms of thermal expansion, magnetization characteristics, and photothermal conversion. For instance, electrothermal-responsive materials including shape memory alloys [36–

 doi:10.20944/preprints202401.2039.v1

38], shape memory polymers [39–41] and twisted fibers/yarns [42–44], are subjected to low thermal-responsive efficiency and low actuation frequency as a result of time-consuming heating and cooling cycles. Although magnetic soft materials have demonstrated their performance in some surgical applications [45–50], achieving high-precision and high-stability operations remain challenging, particularly in reprogrammable design and fabrication of magnetization profiles. Photo-responsive materials employ ultraviolet (UV) irradiation to provide motion energy for actuators [51], but the response characteristics of photo-responsive materials are severely affected by their photothermal conversion efficiency. In addition, the prolonged UV irradiation can damage most interacting objects, especially biological tissues and organs.

In this review, we present a broad range of biomimetic stimuli-responsive materials for soft actuators. Different principles of external stimuli in these responsive materials are first illustrated and discussed, including fluidic, electrical, thermal, magnetic, light and chemical stimuli. Then, state-of-the-art stimuli-responsive materials for soft actuators are summarized, including electroactive polymers, magnetic soft composites, hydrogels, liquid crystal elastomers, shape memory alloys and chemical-responsive materials. In addition, we also compared the mechanical properties of these stimuli-responsive materials. Finally, we discuss opportunities in the field of soft actuators, and highlight the challenges that need to be addressed in order to achieve real-world applications of multifunctional artificial soft actuators.

2. Stimuli-responsive principles of soft actuators

Biomimetic stimuli-responsive soft actuators can be carefully created through selecting or synthesizing desired materials, designing functional structures, and establishing manufacture protocols [7]. By introducing external stimuli such as pressure fluid, electric fields, magnetic fields, thermal fields, illumination, and chemical substances in the design, the biomimetic soft actuators can generate specific strains or deformations. Such deformation is achieved by converting multiple energy inputs into mechanical energy outputs, providing the necessary power. The promising attributes of elastomer/soft materials, such as high flexibility, super-elasticity, viscoelasticity, and hysteresis characteristics, can be fully utilized in driving and controlling biomimetic soft actuators, and further improving the overall performance of soft actuators.

Fluidic stimuli

Fluidic actuation can be categorized into hydraulic actuation and pneumatic actuation. Hydraulic actuation is widely used in traditional industrial robotic arms/hands. Compared to pneumatic actuators, hydraulic actuators offer several advantages, including a large driving force, a high power-to-weight ratio, fast response speed, and low compressibility of the fluid medium [52,53]. While pneumatic actuation is more commonly used driving methods in soft actuators/robots than hydraulic actuation, with two forms of actuation: positive-pressure actuation and negative-pressure actuation. Positive-pressure actuation involves filling the cavities of pneumatic actuators with gas to achieve bending, extending, twisting, and other deformations of the soft actuators. Negative-pressure actuation, on the other hand, involves removing gas inside to create the cavities to shrink and deform, thereby driving the soft actuator to move [54].

Pneumatic network (PN) is a commonly used structure for pneumatic soft actuators, consisting of a driving layer and a strain limiting layer [30,31]. The driving layer is designed with multiple small cavity networks inside a flexible material, while the strain limiting layer is made of non-stretchable or highly elastic modulus materials. The driving layer and the strain limiting layer are sealed through bonding. When driven by positive-pressure gas, the PN actuator bends towards the side of the strain limiting layer. Conversely, when driven by negative-pressure gas, the PN actuator bends towards the side of the driving layer (Figure 1A). The bending performance of PN actuators can be easily improved by adjusting the morphology, wall thickness of cavities, and material characteristics.

 doi:10.20944/preprints202401.2039.v1

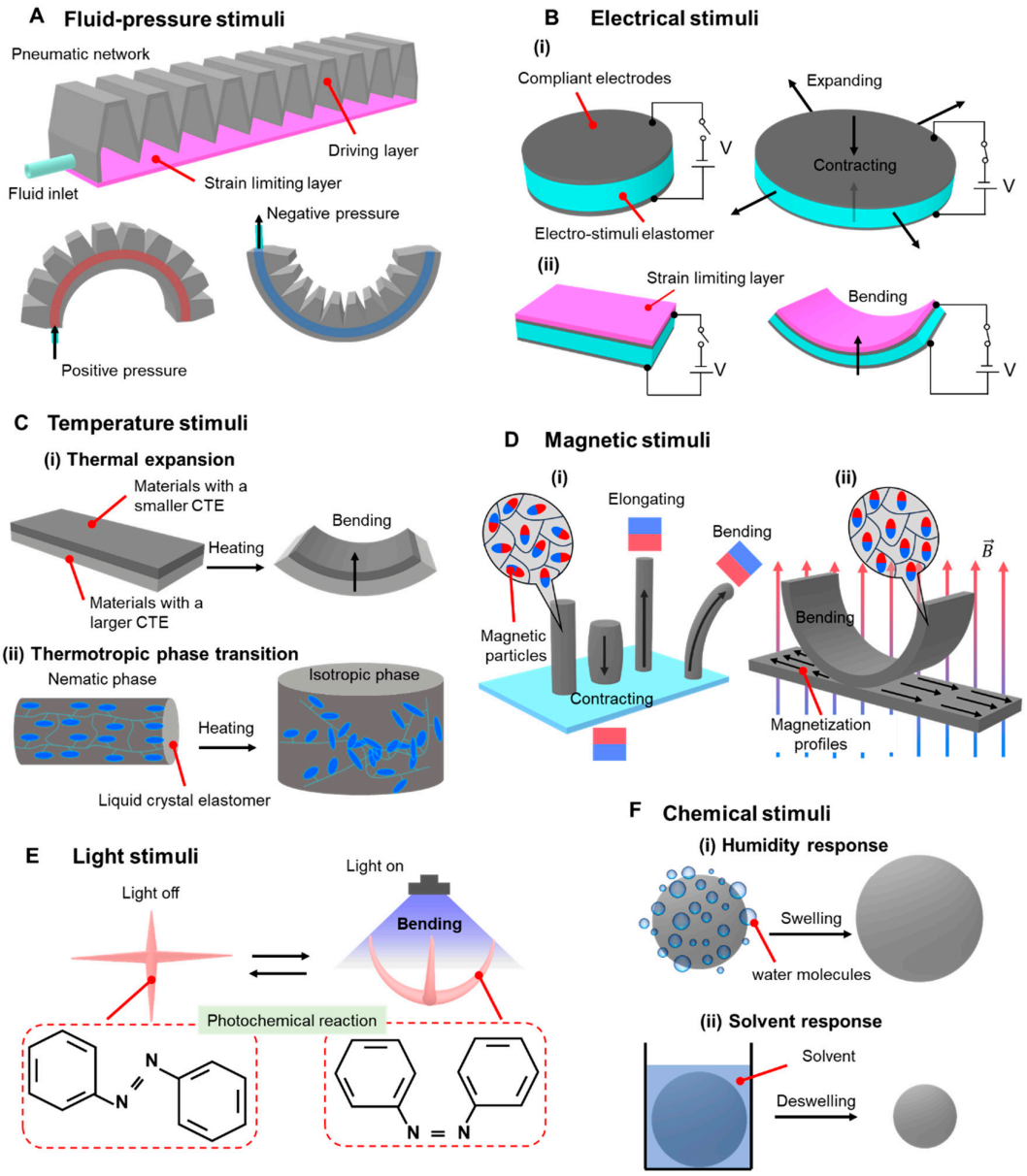

Figure 1. Stimuli-responsive principles of biomimetic soft actuators. **A**. Pneumatic network actuators are actuated by positive-pressure or negative-pressure gas. **B-F**. Actuation mechanisms triggered by external stimuli: electric fields (panel **B**), temperature (panel **C**), magnetic fields (panel **D**), light (panel **E**) and chemical stimuli (panel **F**).

Electrical stimuli

Electrically driven soft actuators are commonly fabricated using electroactive polymers. These polymers are capable to undergo macroscopic mechanical deformations when an electric field is applied to them. One of the most prevalent electroactive polymers is the dielectric elastomer (DE). In a typical design of a DE actuator, as shown in Figure 1B-i, the upper and lower surfaces of the DE film are coated with compliant electrodes, forming a parallel plate capacitor. When a high voltage is applied to these compliant electrodes, opposite charges are generated on both sides of the DE actuator, creating a Maxwell stress that induces the actuator to contract along its thickness direction and increase its area [55–57]. In order to achieve greater strain energy, DE actuators typically require a rigid frame and a pre-tensioning step [58]. Without pre-tensioning, DE actuators have lower output force, smaller strain, and lower energy density, unless they incorporate multi-layer strain-stiffening

 doi:10.20944/preprints202401.2039.v1

elastomers [59] (Figure 1B-ii). Electrically driven soft actuators offer advantages such as high energy density, strong flexibility, fast response rate, and large deformation. As a result, they are widely used in the design of soft robots.

Thermal stimuli

Thermal-responsive soft actuators are primarily based on two types of materials: electrothermal responsive materials and photothermal responsive materials. Electrothermal responsive materials utilize electrical current to generate Joule heating through thermal resistive materials, causing the actuators to expand or contract. Common examples of electrothermal soft materials are shape memory alloys [36–38] and shape memory polymers [39–43]. These thermal-responsive soft actuators are designed to achieve improved performance output and exhibit complex and diverse deformations. To achieve these functions, several effective strategies have been explored, including material anisotropic re-alignment [60], optimization of structural design [61], patterning of material properties using advanced manufacturing techniques [62], mechanically pre-treating the materials [42,43], and integrating multi-layer structures with different coefficients of thermal expansion (CTE) [63,64] (Figure 1C-i).

Liquid crystal elastomers (LCEs) are widely used as photothermal responsive materials due to their inherent anisotropy and ability to undergo reversible actuation with large anisotropic deformations (up to 500% strain). This deformation occurs when LCE materials are heated above a certain temperature, causing the pre-aligned crystalline phase to reorient from anisotropic to isotropic (Figure 1C-ii). By coupling with photomechanical effect, LCEs can achieve complex shape deformations [65]. However, LCE actuators suffer from slow response speed and low driving efficiency, mainly due to the long heating and cooling cycles required [7].

Magnetic stimuli

Soft actuators driven by external magnetic fields are produced by incorporating magnetic micro/nanoparticle fillers (neodymium iron boron and ferroferric oxide) into soft matrix materials (Ecoflex, polydimethylsiloxane, hydrogel). These magnetic soft actuators, as depicted in Figure 1D-i, exhibit deformations such as elongation, contraction, and bending when subjected to external magnetic fields [66]. The unidirectional magnetization technology, typically based on origami structures, is commonly employed to encode the internal magnetization profiles of these magnetic soft actuators. Magnetic soft actuators are firstly folded into predetermined shapes and then magnetized to saturation using a strong unidirectional magnetic field. Consequently, the magnetic soft actuators acquire magnetization profiles that align parallel to the direction of the magnetization field. In recent advances of magnetic responsive materials, Pena-Francesch et al. synthesized a magnetic gel material, which may open new opportunities for soft robotics, medical devices, and sustainable organic magnets [67].

When subjected to a spatially uniform actuation magnetic field, the magnetization profiles of magnetic soft actuators gradually align with the direction of the magnetic field (as shown in Figure 1D-ii). Depending on the specific application, different magnetization profiles are required to achieve different motion modes. By simply folding the magnetic soft actuator into a new shape and magnetizing it again to saturation, new deformation information can be encoded into the actuator.

By modulating the parameters of the external magnetic field (such as amplitude, gradient, and direction) and the magnetization profiles, magnetic soft actuators can achieve multimodal locomotion in various complex environments [68]. They can also exhibit biomimetic movement and functions [27,69], as well as complex deformations [70,71]. The strength of magnetization, driving signals, and overall shapes of the filling materials play crucial roles in determining the deformation modes of magnetic soft actuators. Microscale magnetic soft robots are often designed for applications in enclosed spaces or clustered environments, particularly in interventional medical scenarios [72–75].

 doi:10.20944/preprints202401.2039.v1

Light stimuli

Photo-responsive actuation is advantageous for long-distance and non-contact actuation. Photo-responsive actuators can be controlled by manipulating the size, energy, and wavelength of light sources, allowing for selective response, local response, and spatiotemporal response in photo-responsive soft actuators. In comparison to magnetic soft actuators, light sources can be modulated with higher spatiotemporal resolution using optical choppers, lenses, and photomasks [76].

The working principles of photo-responsive actuators primarily rely on the mechanisms of photothermal effect, photoelectric conversion, and photochemical reactions (Figure 1E). When exposed to light, these actuators can undergo macroscopic deformations and motions owing to their unique characteristics in various photo-responsive materials such as carbon-based materials, gel materials, and liquid crystal materials [77–80]. These materials exhibit specific features including shape memory [81,82], photothermal strain [83,84], photothermal adsorption and desorption [85–88], photothermal tension [89], photoisomerization [90–92], and photomagnetic properties [93,94], which enable their responsiveness to light stimuli. Currently, photo-responsive actuators mainly utilize photothermal expansion, photothermal adsorption or desorption, and photothermal Marangoni effect [95,96] to achieve controlled and reversible deformations and motions. These mechanisms hold great potential for a wide range of applications.

Chemical stimuli

Chemical-responsive actuation is a type of contact-responsive actuation method that involves direct contact between stimuli sources and soft actuators. This method allows for highly sensitive and rapid response speeds. Chemical substances are able to penetrate into the interior of the soft actuators, leading to significant deformations. Some common examples of chemical stimuli sources include water, volatile solvents, salt solutions, and acid-base solutions. When these substances come into contact with the soft actuators, they can induce various types of deformations and motions. This makes chemical-responsive actuation a versatile and powerful approach for a range of applications.

Humidity-responsive actuators are a type of contact-responsive actuation method that is triggered by water molecules. These actuators are made of materials that contain a high number of hydrophilic oxygen-containing functional groups, which can reversibly adsorb or de-adsorb water molecules [77]. This adsorption or de-adsorption process leads to changes in the molecular gaps within the materials, resulting in the expansion or contraction of humidity-responsive actuators (Figure 1F-i). When the surrounding humidity increases, humidity-responsive actuators made of hydrophilic materials absorb moisture and expand. Conversely, when the surrounding humidity decreases, the actuators shrink as moisture detaches from the materials [97]. This reversible response to changes in humidity makes humidity-responsive actuators useful in various applications.

Solvent-responsive soft actuators are designed to selectively adsorb volatile chemical solvents such as acetone, ethanol, and tetrahydrofuran. These solvents can penetrate into the interior of the actuators and induce rapid and reversible deformation due to anisotropic volume changes (Figure 1F-ii) [98–100]. This property makes solvent-responsive actuators useful in applications where a specific solvent needs to be detected or controlled.

pH-responsive soft actuators are capable of sensing changes of pH values in the surrounding environment. These actuators are primarily designed for operation in liquid environments [101]. They can undergo structural changes, such as expansion or contraction, in response to variations in pH levels. This pH sensitivity enables these actuators to be used in applications where pH changes need to be monitored or utilized for actuation purposes.

3. Stimuli-responsive materials for soft actuators

The application advances of representative stimuli-responsive materials for soft actuators will be discussed in this section. These materials mainly include electroactive polymers, magnetic soft composites, hydrogels, liquid crystal elastomers, shape memory alloys and chemical-responsive materials. The physical properties and stimuli-responsive performance of these typical materials with

 doi:10.20944/preprints202401.2039.v1

distinct activation mechanisms are summarized in Table 1. We noticed that these materials have a Young's modulus ranging from <100 kPa to >2 GPa, and that the response time varies from ~1 ms to >100 s depending on the stimuli method. In addition, the functioning durability also vastly tested with <10 cycles to >10^5 cycles. Based on their stimuli methods, we discuss each of these soft materials as follow.

Electroactive polymers

Electroactive polymers (EAPs) are polymers that exhibit high power density and remarkable mechanical compliance, making them suitable for simulating artificial muscles. These polymers can be categorized into two types based on their action mechanisms: ionic electroactive polymers and electronic electroactive polymers [102,103].

Ionic EAPs, including conductive ionic gels, conductive polymers and polymer-metal mixtures, have been used to fabricate soft actuators. These materials exhibit asymmetric volume expansion near the electrodes due to ion diffusion. The advantage of ionic EAPs is that they only require a low voltage of 1~2 V to generate a large deformation. However, maintaining constant deformation can be challenging due to the presence of electrolytes [104–106].

Table 1. Performance comparison of typical stimuli-responsive materials for soft actuators.

Materials	Stimulus sources	Response time	Mechanical properties	Crosslinking methods	Durability	Refs
Ecoflex 00-30	Fluidic stimuli	~50 ms	E=~0.1MPa	Thermal curing	1×10^5 cycles	[30]
IPMCs	Electrical stimuli	~20-90 s	NA	Ionic crosslinking	NA	[104]
IGMN	Electrical stimuli	~50 s	E=~0.35MPa	Ionic crosslinking	7.6×10^4 cycles	[105]
PEDGA, PEDOT: PSS	Electrical stimuli	~0.8 s	E=~11-15MPa	Ionic crosslinking	5×10^3 cycles	[107]
PDMS	Electrical stimuli	~1.67 ms	E=~4 MPa	Thermal curing	NA	[35]
PDMS	Electrical stimuli	5 ms	NA	Thermal curing	5×10^4 cycles	[113]
FSNPs, Ecoflex 00-30	Electrical stimuli	1.43 ms	G= 27-979 kPa	Thermal curing	2.6×10^5 cycles	[116]
Fe_3O_4 nanoparticles, Fe-alginate, PAAm	Magnetic stimuli	NA	τ= 200–1000 kPa	Ionic crosslinking	NA	[120]
Carbonyl iron microparticles, TPU	Magnetic stimuli	25 ms	NA	Thermal curing	NA	[121]
NdFeB microparticles, Ecoflex 00-10	Magnetic stimuli	NA	E=~78.6 ± 4.8kPa	Thermal curing	NA	[67]
Iron microparticles, PDMS	Magnetic stimuli	35.8 ms	E=~2 MPa	Thermal curing	5×10^3 cycles	[68]
NdFeB, FSNPs, Ecoflex 00-30 Part B, SE 1700	Magnetic stimuli	~0.1 s	G=330 kPa	Thermal curing	NA	[130]
PEG_{1000}, HDI, HABI	Light stimuli	~35 s	τ=2.88 MPa	Light-crosslinking	500 cycles	[142]
BN, AlN, Si_3N_4, NIPAM	Light stimuli	~30 s	E=9.71 ± 0.06 kPa	Photopolymerization	> 10 cycles	[144]
PNIPAAM, AuNPs, rGO	Light stimuli	< 1 s	τ= 8–18 kPa	Photopolymerization	NA	[148]
RM 257, HDT	Light stimuli	< 0.2 s	τ= 3–4 MPa	Light-crosslinking	1×10^6 cycles	[162]
PLCMs, MDI, HEMA	Light stimuli	4-8 s	E=~11-20 MPa	Light-crosslinking	NA	[165]
Ni, Cr, SMP	Electrothermal stimuli	20 s	E=~3.33-125.65 MPa	NA	NA	[166]
Graphene oxide, SU-8	Humidity stimuli	~22-26 s	τ=~30-90 MPa	Photopolymerization	> 500 cycles	[177]
PVDF, PPy	Solvent stimuli	3.1-9.2 s	E=~2.53 GPa	Thermal curing	NA	[180]
PAAc	pH stimuli	~120 s	E=~300 MPa	Photopolymerization	> 10 cycles	[184]

E, Young's modulus; G, shear Modulus; τ, ultimate stress; NA, not applicable; Ecoflex, a silicone rubber; PDMS, polydimethylsiloxane; IPMCs, ionic polymer–metal composites; IGMN, ionic gel/metal nanocomposite; PEDGA, poly(ethylene glycol) diacrylate; PEDOT:PSS, poly(3,4-ethylenedioxythio-phene)-poly(styrenesulfonate); DEs, dielectric elastomers; FSNPs, fumed silica nanoparticles; PAAm, polyacrylamide; TPU, thermoplastic polyurethane; NdFeB, neodymium–iron–boron; SE 1700, a silicone-based material; PEG_{1000}, polyethylene glycol; HDI, hexamethylene diisocyanate; HABI, a tetrahydroxy functionalized crosslinker; BN, boron nitride; AlN,

 doi:10.20944/preprints202401.2039.v1

aluminum nitride; Si_3N_4, silicon nitride; NIPAM, n-isopropylacrylamide; PNIPAAM, poly(N-isopropylacrylamide); AuNPs, gold nanoparticles; rGO, reduced graphene oxides; RM 257, a liquid crystal mesogen; HDT, hexane dithiol; PLCMs, polymerizable liquid crystal monomers; MDI, diphenylmethane diisocyanate; HEMA, 2-Hydroxyethyl acrylate; SMP, shape memory polymer; SU-8, a type of photoresist; PVDF, polyvinylidene difluoride; PPy, polypyrrole; PAAc, Poly(acrylic acid).

Researchers have made progress in developing advanced ionic EAPs soft actuators. For example, Park et al. designed a five-layer structured soft actuator using ionic EAPs, where the porous intermediate layer improves the electromechanical performance and charging capacity [107]. This soft actuator can generate crimping, crawling, and bending behaviors under low voltage. They also created a spider-shaped soft actuator that can move back and forth, demonstrating potential applications such as smart switches (Figure 2A). Ma et al. developed ionic soft actuators based on perfluorosulfonic acid with high-quality Pt electrodes using a chemical coating method assisted by isopropanol [117]. The Pt electrodes significantly enhance the driving performance of the ionic actuators, enabling a low driving voltage of 1 V, a deforming amplitude of up to 35.3 mm, a response frequency of up to 10 Hz, and a bending degree of up to 596.2 ° s-1. These exceptional features allow the soft actuator to mimic the blooming of a forsythia flower, the coiling behavior of a cucumber tendril, and the high-frequency wing flapping of a dragonfly (Figure 2B).

Electronic EAPs soft actuators are commonly designed as a sandwich structure, where the EAP materials are placed between two electrodes. These actuators typically require a high voltage input in order to generate a high mechanical energy density. When a high electric field is applied, the EAP materials undergo expansion along the area direction and contraction along the thickness direction, which is a result of Maxwell stress [108]. Among the various types of electronic EAPs, soft actuators made from dielectric elastomers (DEs) exhibit several advantages such as higher energy density, faster response speed, better driving stability, and larger driving force [109]. However, conventional DE actuators often require a higher driving voltage due to their relatively low dielectric coefficient. Currently, extensive research efforts are focused on enhancing the dielectric constant of DEs and improving their dielectric breakdown strength. Additionally, reducing the elastic coefficient and driving voltage are also key areas of interest [110–112].

In the study conducted by Gu et al., a soft wall-climbing robot was developed using artificial muscles made of DEs. The robot demonstrated the ability to climb vertical wooden walls at a 90° angle while carrying a 10-g payload (Figure 2C). It was also capable of carrying cameras to capture videos in vertical tunnels, adjusting its body height to navigate through confined spaces, and following labyrinth-like trajectories on a flat surface [32]. Although DE actuators exhibit a small driving force due to their biaxial strain response behavior, there are two commonly used methods to convert this behavior into linear motion. One approach involves stacking multiple layers of DE films, while the other involves folding a single layer into multiple layers of DE films [113–115]. Wang et al. proposed a soft crawling robot that utilized reconfigurable DEs with chiral grid feet (Figure 2D). This robot was capable of rapidly switching between forward, backward, and circular motions by adjusting the frequency of the input voltage. It also demonstrated the ability to reconstruct its structure under external temperature stimulation [185]. Li et al. developed a wireless self-powered soft robot using DEs that was inspired by a deep-sea fish called *Pseudolaris swirei*. This robot was designed for deep-sea exploration and was tested at depths of 10,900 meters in the Mariana Trench and 3,224 meters in the South China Sea (Figure 2E). The tests confirmed that the robot exhibited excellent pressure resistance and swimming performance, showcasing its suitability for deep-sea exploration [186].

In recent years, 3D printing techniques, specifically direct ink writing, have been widely employed to fabricate DE actuators with complex structures that enable three-dimensional motions. For instance, Lewis et al. utilized 3D printing to create coaxial 3D fiber bundles and Janus-shaped coils. These coil actuators, when subjected to a voltage, bent towards the fiber side of the dielectric elastomer, enabling intricate and controllable driving behavior [116]. Additionally, Chortos et al. used 3D printing to develop a high-precision cross-shaped DE actuator capable of generating a 9%

 doi:10.20944/preprints202401.2039.v1

in-plane contraction [57]. Such advancements in 3D printing technology have significantly contributed to the development of DE actuators with complex structures and improved functionality.

Piezoelectric materials are also commonly employed in electrically driven soft actuators, enabling the conversion of electrical energy into mechanical force. Specifically, when a piezoelectric material is exposed to a specific electric field, it induces mechanical deformation or pressure along a particular direction. Soft actuators based on piezoelectric materials harness the inverse piezoelectric effect to generate force by converting electrical energy into mechanical force. Recently, piezoelectric actuators have attracted much attention in the field of soft robotics owing to their advantages of high accuracy, fast response, high driving frequency, and lightweight [187–189].

The piezoelectric coefficient of organic flexible piezoelectric materials is generally lower than that of conventical rigid piezoelectric ceramics. However, organic piezoelectric materials are still considered the preferred choice for piezoelectric actuators because of their remarkable flexibility and ease of preparation. These materials offer advantages in terms of conformability, lightweight, and the ability to integrate into various shapes and structures, making them well-suited for applications requiring soft and flexible actuation. Currently, several flexible piezoelectric materials, such as polyvinylidene fluoride (PVDF) [190,191], polyurea [192,193], and peptides [194,195], have been widely utilized in the development of soft actuators. For instance, Wu et al. [196] developed an insect level soft robot using PVDF, which runs at a very fast speed and can reach up to 20 body lengths per second (Figure 2F). Furthermore, Liang et al. [197] further enhanced the functionality of soft robots by incorporating two electrostatic foot pads. This addition enabled the soft robot to achieve precise directional control. In their research, they utilized piezoelectric thin films as the main body, allowing the robot to navigate through mazes with flexibility [Figure 2G]. Moreover, by equipping gas sensors, this soft robot holds significant potential for detecting gas leaks.

Organic flexible piezoelectric materials have gained significant interest in the realm of soft robotics owing to their exceptional electromechanical properties. Nevertheless, the limited deformation amplitude and high actuation voltage pose challenges to their widespread application. Consequently, future research on piezoelectric soft actuators will concentrate on developing wireless strategies and low-voltage piezoelectric materials. These advancements will enhance the performance and expand the potential applications of piezoelectric materials in soft actuators.

 doi:10.20944/preprints202401.2039.v1

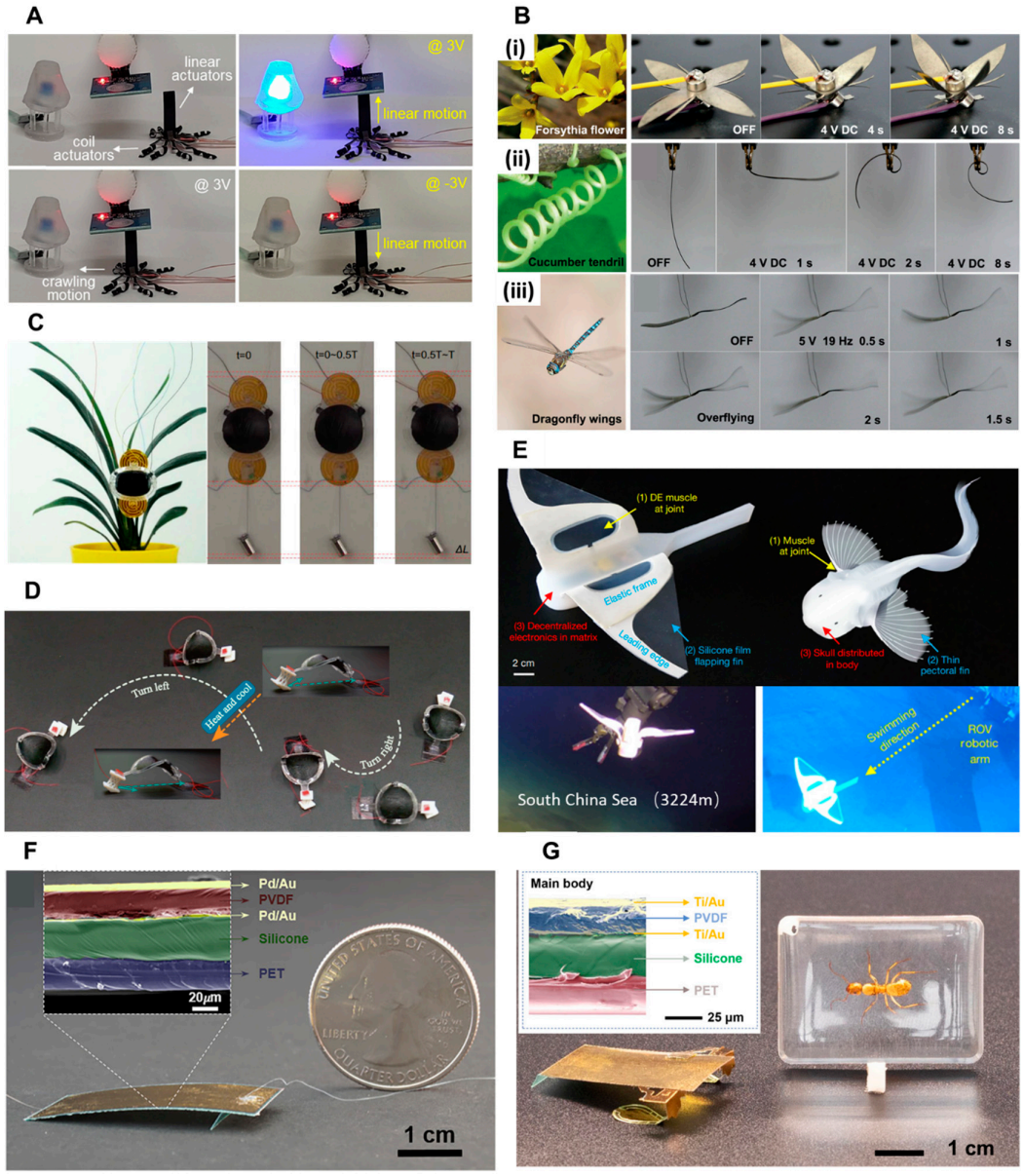

Figure 2. Biomimetic soft actuators based on electroactive polymers. **A**. A spider robot based on ionic EAPs carries a linear actuator to switch on/off of LED bulbs (Reprinted with permission from Ref. [107]. Copyright 2021, American Chemical Society). **B**. Ionic EAPs actuators mimic blooming of forsythia flower, coiling behavior of cucumber tendril and high-frequency wing flapping of a dragonfly (Reprinted with permission from Ref. [117]. Copyright 2019, John Wiley and Sons). **C**. A soft wall-climbing robot based on DEs artificial muscles (Reprinted with permission from Ref. [32]. Copyright 2018, the American Association for the Advancement of Science). **D**. A soft crawling robot based on reconfigurable DEs chiral grid feet (Reprinted with permission from Ref. [185]. Copyright 2023, Springer Nature). **E**. A wireless self-powered DEs soft robot was used for deep-sea exploration in South China Sea and Mariana Trench (Reprinted with permission from Ref. [186]. Copyright 2021, Springer Nature). **F**. An insect level soft robot based on PVDF film (Reprinted with permission from Ref. [196]. Copyright 2019, the American Association for the Advancement of Science). **G**. A piezoelectric driven soft robot with electrostatic footpads (Reprinted with permission from Ref. [197]. Copyright 2019, the American Association for the Advancement of Science).

 doi:10.20944/preprints202401.2039.v1

Magnetic soft composites

According to the magnetization characteristics of magnetic materials, there are three main types: soft magnetic materials, hard magnetic materials, and superparamagnetic materials. Soft magnetic materials, such as iron, nickel, and silicon-based ferroalloys, possess high magnetic susceptibility and relatively low residual magnetism and magnetic coercivity [66]. When it comes to constructing magnetic soft robots using isotropic soft magnetic materials, it is challenging to achieve gait motions or gripping operations. This is because isotropic spherical soft magnetic particles do not have a preferred magnetization direction. As a result, the magnetic moment they receive is always parallel to the external magnetic field, leading to zero overall torques within the soft magnetic composites.

Magnetic soft actuators made of soft magnetic soft composites could achieve simple deformations such as overall shortening, elongating, and bending by utilizing the magnetic attraction of nonuniform magnetic fields on magnetic particles [118–120]. In order to generate effective magnetic torque in soft magnetic materials, it is necessary to introduce some form of magnetic anisotropy to disrupt the symmetry of the soft magnetic material's response to external magnetic fields. One approach is to build anisotropic magnetic particle chains inside magnetic soft composites to achieve overall anisotropy at the composite level [121,122] (Figure 3A). Another approach is to use anisotropic soft magnetic materials, such as rod-shaped [123,124] or sheet-shaped particles [125,126], to achieve local asymmetry at the magnetic particle level (Figure 3B). These strategies enable the soft magnetic actuators to exhibit more complex and controllable motions.

Hard magnetic materials are known for their strong anti-demagnetization ability and high residual magnetism. Some commonly used hard magnetic materials include hexagonal ferrite barium ($BaFe_{12}O_{19}$) and hexagonal ferrite strontium ($SrFe_{12}O_{19}$), which have a magnetic coercivity of up to 300 kA/m. Additionally, materials like samarium cobalt ($SmCo_5$, Sm_2Co_{17}) and neodymium iron boron ($Nd_2Fe_{14}B$) exhibit even higher magnetic coercivity, exceeding 1000 kA/m [66,127–129]. These materials are widely utilized for applications that require strong and stable magnetic properties.

Magnetic soft composites, which are created by incorporating hard magnetic particles into soft polymer matrix materials, possess both hard magnetic properties and exceptional mechanical flexibility. Once these composites are magnetized to saturation, the residual magnetism remains relatively constant regardless of the driving magnetic fields within the range of their magnetic coercivity [66]. The magnetization profiles of hard magnetic soft composites can be specifically designed to achieve desired deformations, regardless of the shape and orientation of the hard magnetic particles (Figure 3C) [67]. This capability allows for the development of impressive hard magnetic soft actuators that can undergo reconfigurable and multi-dimensional deformations. Advanced manufacturing technologies, such as 4D printing techniques, have been utilized to manufacture diverse magnetization profiles (Figure 3D) [130], enabling the creation of complex and customizable actuator designs [131,132]. These advancements in manufacturing techniques have expanded the possibilities for designing and fabricating innovative hard magnetic soft actuators with a wide range of deformations.

When the size of soft magnetic materials is reduced to a critical size, the magnetic coercivity starts to decrease rapidly until there is no residual magnetism or magnetic coercivity left. Such soft magnetic materials are called as superparamagnetic materials [66]. By incorporating chained superparamagnetic particles into magnetic soft composites, the overall magnetic anisotropy can be achieved, making it an effective approach for manufacturing magnetic soft actuators [122,133,134]. However, the loading capacity of superparamagnetic materials in soft matrix materials is generally lower than that of pure soft or hard magnetic materials [135,136]. This is because superparamagnetic particles are prone to agglomeration due to van der Waals forces [137–139]. This limitation needs to be considered when designing and fabricating magnetic soft composites using superparamagnetic materials.

To enhance the dispersibility of magnetic nanoparticles, polymers are often employed to coat or functionalize them, resulting in the formation of core-shell structures. This approach enables intergranular electrostatic repulsion, which helps to balance out the van der Waals attraction between magnetic nanoparticles [140]. However, when compared to other types of magnetic soft composites,

 doi:10.20944/preprints202401.2039.v1

the magnetization profiles per unit volume within magnetic soft actuators based on superparamagnetic materials are lower. This is primarily due to the lower concentration of magnetic particles in these composites. As a result, the magnetic torques or forces generated by these actuators are smaller, resulting in less pronounced magnetic hardening, elongation, shortening, and bending effects.

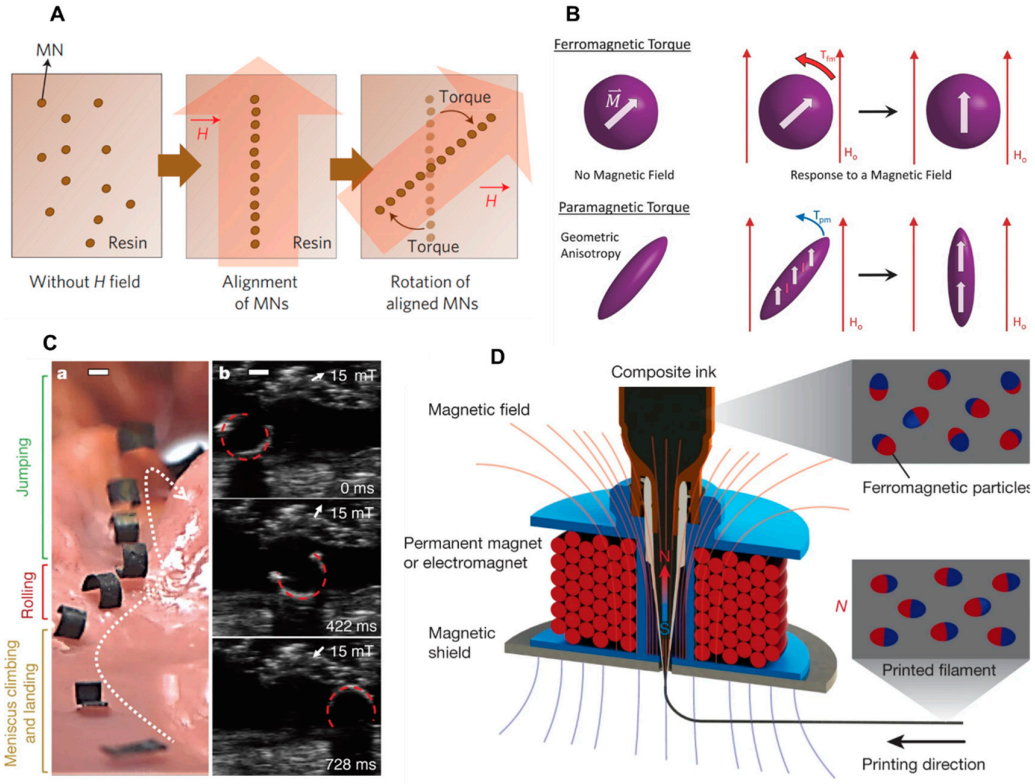

Figure 3. Magnetically responsive materials for biomimetic soft actuators. **A**. Build anisotropic soft magnetic particle chains inside magnetic soft composites (Reprinted with permission from Ref. [122]. Copyright 2011, Springer Nature). **B**. Employ anisotropic soft magnetic materials such as rod-shaped and sheet-shaped to achieve local asymmetry (Reprinted with permission from Ref. [123]. Copyright 2016, John Wiley and Sons). **C**. Magnetic soft robot fabricated with hard magnetic materials navigating across a synthetic stomach phantom (Reprinted with permission from Ref. [67]. Copyright 2018, Springer Nature). **D**. Hard magnetic particles embedded in the composite ink are reoriented by the applied magnetic field around the dispensing nozzle (Reprinted with permission from Ref. [130]. Copyright 2018, Springer Nature).

Hydrogels and Liquid crystal elastomers

Hydrogels are polymer materials with three-dimensional cross-linked networks that are highly hydrated. They are known for their excellent biocompatibility and high-water content. The mechanical properties and responsiveness of hydrogels can be adjusted over a wide range via incorporating various functionalities into photo-responsive biomimetic systems. These unique characteristics make hydrogels ideal for use as intelligent responsive materials in important fields such as soft robotics, artificial muscles, and nanogenerators [141].

There are two main methods for fabricating hydrogel soft actuators. One approach involves creating a hydrogel actuator with a uniform surface and then applying uneven light stimuli to induce structural deformations. For example, Xiang et al. developed a polyurethane (PU) hydrogel actuator with a uniform composition to achieve anisotropic deformations [142]. When exposed to light, the PU hydrogel actuator undergoes deformations such as expansion and bending. These deformations

 doi:10.20944/preprints202401.2039.v1

occur due to the decrease in cross-linking reactions and an increase in hydrophilicity on the illuminated side. By adjusting the position of the light source, the PU hydrogel actuator can exhibit curling, twisting, and folding motions (Figure 4A). This method allows for precise control and manipulation of hydrogel actuators, enabling a wide range of motion possibilities for various applications.

Another approach is to construct hydrogel actuators with heterogeneous structures using various fabrication techniques such as stepwise synthesis, photolithography, 3D printing, ion-patterned crosslinking, magnetic/electric field induction and micro-assembly [143–148]. For instance, Hou et al. developed a hydrogel-based vehicle that can follow the direction of photon illumination and the internal direction to adjust the unconstrained fluid space [149]. By manipulating customized photothermal nanoparticles and micro pores in polymer matrices, strong chemical mechanical deformation of soft materials was achieved (Figure 4B). Chen et al. developed a gradient hydrogel actuator with exceptional mechanical performance and durability [150]. This actuator enables several applications in underwater soft robotics for concept verification. Examples include simulating the opening and closing of flowers in water under near-infrared light, manufacturing light-driven soft grippers for grasping, lifting, and releasing objects, as well as achieving photodynamic underwater movement of crawling robot on the directional ratchet surface (Figure 4C). These heterogeneous hydrogel structures offer advanced functionalities and expand the possibilities for developing innovative soft robotic systems with enhanced performance and adaptability.

Liquid crystal elastomers (LCEs) are a unique class of polymers that combine liquid crystal polyacrylates with the main or side chains of the polymer structure. They are characterized by excellent mechanical properties, self-healing, shape memory and fast reaction. By adjusting the orientation of liquid crystal molecules and the elastic entropy of polymers, soft actuators based on liquid crystal elastomers can achieve various deformation modes such as expanding, contracting, curling and twisting [151–155]. In addition, adding photothermal materials to LCEs can convert light energy into thermal energy, thereby inducing LCEs phase transition and producing deformations [156–159].

LCEs actuators are mainly based on photochemical response and photothermal response [160–163]. Zhao et al. mixed liquid crystal Diels Alder networks (LCDANs) loaded with carbon nanotubes (CNTs) to prepare twisted fibers. Based on this, a spring-type CNTs-LCDANs soft actuator further was manufactured by controlling the winding direction of the twisted fibers [164]. In their study, the CNT-LCDANs actuator can achieve rolling with a speed of 22 mm/s in various environments (e.g. water and beach) under continuously light stimulus (Figure 4D). In addition, Song et al. manufactured a photo-driven actuator by covalently crosslinking polyurethane (PU) into a LCE network (PULCN) [165]. In particular, by constructing a cross-linking density gradient on the thickness of the membrane, the PULCN actuator exhibits programmable initial shapes under a local and sequential near-infrared light (Figure 4E).

 doi:10.20944/preprints202401.2039.v1

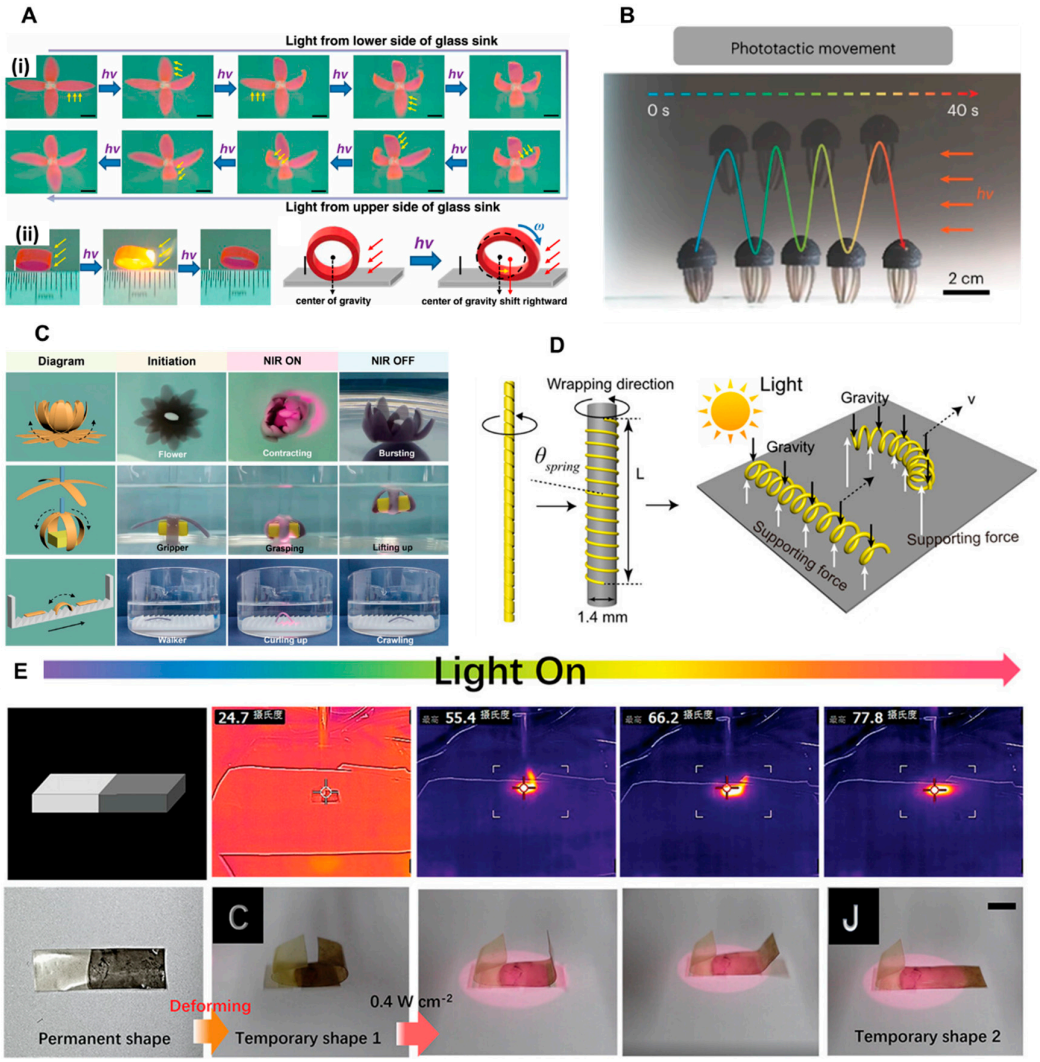

Figure 4. Photo-responsive materials for biomimetic soft actuators. **A**. Localized photo-driven closing and blooming of biomimetic flower and photo-driven forward rolling of a wheel based on PU hydrogels (Reprinted with permission from Ref. [142]. Copyright 2021, Elsevier Ltd.). **B**. A hydrogel-based vehicle that can follow the direction of photon illumination (Reprinted with permission from Ref. [149]. Copyright 2023, Springer Nature). **C**. Opening and closing of flowers, soft grippers to grasp, lift and release goods, and soft robot to crawl on the surface of the directional ratchet in the water under near-infrared light (Reprinted with permission from Ref. [150]. Copyright 2022, John Wiley and Sons). **D**. A spring-type LCEs fiber actuator capable of controlling the winding direction of twisted fibers (Reprinted with permission from Ref. [164]. Copyright 2021, American Chemical Society). **E**. A LCEs soft actuator driven by local and sequential light with near-infrared photo-responsive polydopamine (Reprinted with permission from Ref. [165]. Copyright 2023, John Wiley and Sons).

Shape memory alloys

Based on the deformation principle of shape memory alloy (SMA), a series of SMA-driven worm-like actuators/robots are developed to mimic the peristalsis, crawling and rolling of worms and geometries. The manufacturing methods of SMA-driven actuators is to embed SMA springs into soft polymers. By applying electrical current to heat SMA springs for deformations, the polymer body passively deformed owing to deformations of SMA springs. Robot's wedge-shaped legs generate sufficient friction to obtain appropriate movement through the deformation of the body.

Sangok et al. developed a mesh-like soft crawling robot (Meshworm) that mimics the peristaltic movement of earthworms [38]. In their research, the longitudinal SMA spring can shorten or bend

 doi:10.20944/preprints202401.2039.v1

the Meshworm, while the circumferential SMA spring contracts, which further causes Meshworm to elongate axially. Wu et al. [166] developed 3D-printed and origami robots that utilize SMA wires (Figure 5A). These robots were designed with "knitting-constraints" and ridden using the SMA wires. In their experiments, the average speed achieved by the 3D-printed robot was 20 mm/min, while the origami robot had an average speed of 15 mm/min. This study demonstrates the use of SMA wires in robotic systems and shows the capability of the 3D-printed and origami robots to achieve controlled motion within a certain displacement range and at different speeds. Hyun-Taek et al. [167] proposed a small SMA soft composite actuator prepared by two-photon printing. As shown in Figure 5B, the deformation mode can be changed by changing the direction of the support lamination, and the driving can be controlled by the local electric heating effect of the carbon nanotube layer deposited inside the driver. This micro actuator can generate a force of 390 μN and achieve a bending angle of up to 80°, demonstrating the ability to lift and grip objects using single and double arm devices [167].

Liang et al. [168] developed a novel flexible self-healing robot driven by miniature bidirectional SMA springs (Figure 5C). This self-healing robot is driven by a new type of bidirectional shape memory alloy (TWSMA) spring actuator, with a crawling speed of 21.6 centimeters per minute, equivalent to 1.57 body lengths per minute. In addition, Zheng et al. [169] proposed a non-adhesive origami soft actuator (OSA) (Figure 5D). These OSA devices are composed of three key components: an SMA wire for generating driving force, a printing heater for thermal stimulation, and an elastic origami structure for providing restoring force. The printing heater used in this study has a length of 288 mm and is capable of maintaining a stable driving temperature of 105.1°C when an applied voltage of 6.5 V is supplied. The printing heater plays a crucial role in activating the SMA wire by providing the necessary thermal energy for its shape memory effect. SMA actuators typically require large electrical current for heating and a longer time for cooling, which results in longer response times and significant hysteresis.

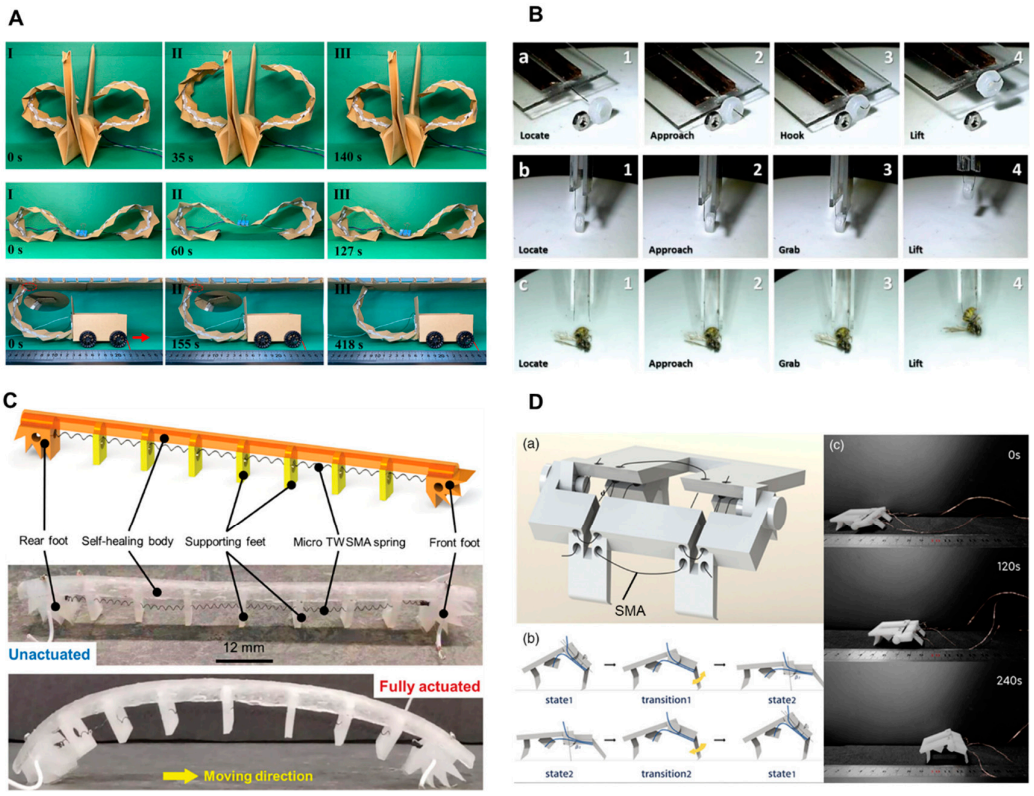

Figure 5. Shape memory alloy for biomimetic soft actuators. **A**. Origami robots based on utilize SMA wires (Reprinted with permission from Ref. [166]. Copyright 2022, John Wiley and Sons). **B**.

 doi:10.20944/preprints202401.2039.v1

Microscale SMA-based soft actuators fabricated by two-photon printing (Reprinted with permission from Ref. [167]. Copyright 2020, John Wiley and Sons). **C**. A flexible self-healing robot driven by miniature bidirectional SMA springs (Reprinted with permission from Ref. [168]. Copyright 2024, John Wiley and Sons). **D**. A non-adhesive origami SMA soft actuator (Reprinted with permission from Ref. [169]. Copyright 2022, John Wiley and Sons).

Chemical-responsive materials

Chemical-responsive materials used in biomimetic soft actuators mainly include humidity-responsive materials, solvent-responsive materials and pH-responsive materials. Humidity-responsive materials generally contain a large number of hydrophilic oxygen-containing functional groups that can reversibly adsorb or de-adsorb water molecules, causing the molecular gaps of humidity-responsive materials to increase or decrease, thereby causing humidity-responsive soft actuators to expand or contract [97].

Graphene oxide (GO) is a typical humidity-responsive material that is widely used in humidity-responsive soft actuators [170–177]. For example, Ma et al. used soft lithography technology to prepare a double-layer structure of GO/SU-8 actuator. When the ambient humidity increased, the GO/SU-8 driver bent towards the SU-8 side [177]. By adjusting the SU-8 pattern, the actuator can achieve controllable deformation (Figure 6A). Although this multi-layer actuator has high deformation degree and rapid response, but there is a problem of interlayer delamination. A feasible approach is to fill or modify other materials in the matrix material to create a gradient in the thickness direction of the matrix material. For instance, Han et al. utilized a magnetic field to create a concentration gradient of Fe3O4 in the thickness direction of the GO film [178], constructing a multi-responsive actuator. In addition, the GO-based actuator prepared by Qiu et al. has different surface morphologies on both sides. When the humidity increases, the GO-based actuator can bend towards the flat side [179].

Solvent-responsive materials used for soft actuators include liquid crystal polymers, hydrogels and semi-crystalline polymers [98–100]. For example, Yim et al. polymerized polypyrrole (PPy) on hydrophobic PVDF membranes via gas-phase polymerization to prepare solvent-responsive actuators. As shown in Figure 6B, the solvent-responsive PVDF/PPy actuators can be used to mimic leaves and flower petals, respectively, under the acetone stimulus [180]. In addition, Wang et al. prepared single-layer asymmetric PVDF actuators by vacuum hot pressing technology. Under acetone stimulus, directional and asymmetric expansion can be generated, and biomimetic behaviors such as entanglement and jumping can be achieved [181].

PH-responsive materials used to prepare actuators have ionizable groups (amine, pyridine and carboxyl) [101,182]. For example, polyacrylic acid (PAAc) contains a large number of carboxyl groups. When the environmental pH increases, the PAAc colloids expand owing to the ionization increase of the PAAc chain. On the contrary, when the environmental pH decreases, PAAc colloid contracts [183]. Based on PAAc materials, Cho et al. used electrospinning technology to fabricate a pH-responsive actuator with a bilayer structure [184]. As shown in Figure 6C, the pH-responsive actuator curled into a tubular shape as the pH increased to 13. The pH-responsive actuator returned to a flattened state as the pH returned to 1. In addition, polyethylene glycol fatty acid ester patterns were selectively modified on the surface to effectively control the deformation direction of the pH-responsive actuator.

 doi:10.20944/preprints202401.2039.v1

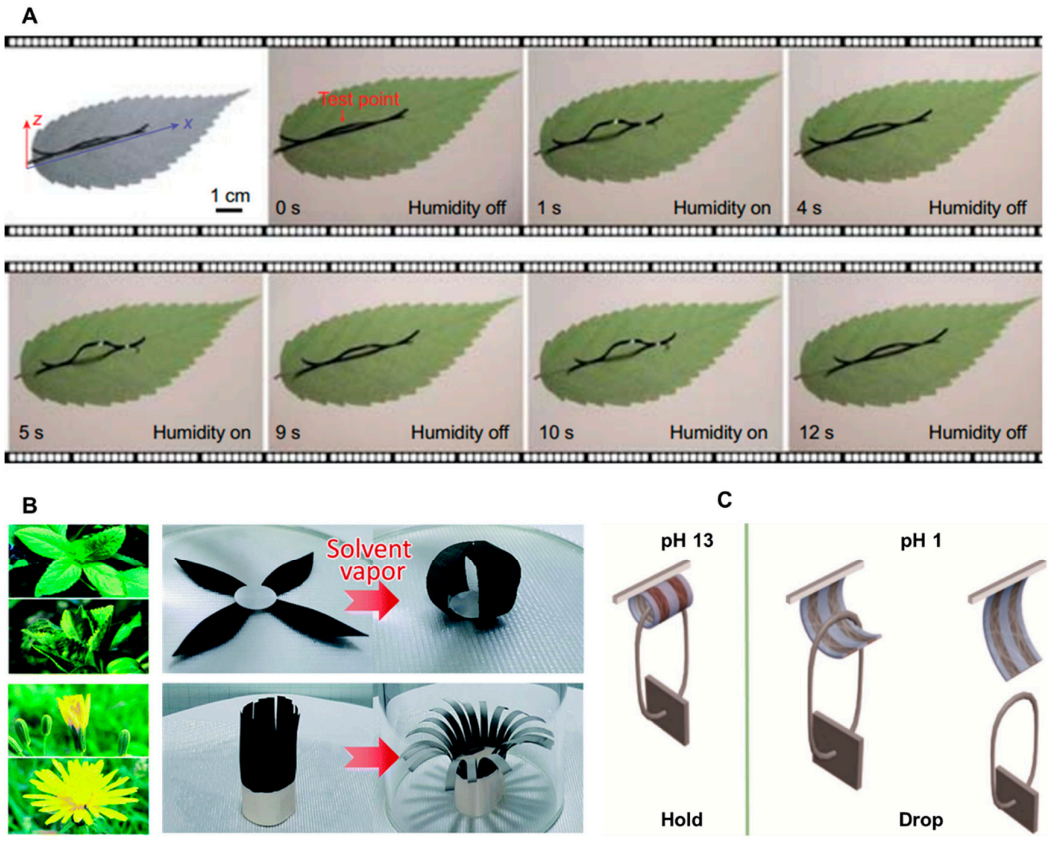

Figure 6. Chemical-responsive materials for biomimetic soft actuators. **A**. The humidity-responsive GO/SU-8 actuator with light weight (Reprinted with permission from Ref. [177]. Copyright 2020, Oxford University Press). **B**. The solvent-responsive PVDF/PPy actuators can be used to mimic leaves and flower petals, respectively, by acetone stimulus (Reprinted with permission from Ref. [180]. Copyright 2021, the Royal Society). **C**. A pH-responsive actuator can curl into a tubular shape as the pH increases to 13 and restore to a flattened state as the pH decreases to 1 (Reprinted with permission from Ref. [184]. Copyright 2022, Elsevier Ltd.).

4. Conclusions and outlook

In this review, we summarized different stimuli methods, which cause responsive soft materials to regulated deform and form soft actuators. In addition, the underlying mechanisms to cause stimuli-response for different actuator materials were also introduced, including fluidic, electrical, thermal, magnetic, light and chemical stimuli. Corresponding to each stimulus, we further concluded 6 types of stimuli-responsive soft matters, and discussed >20 different materials worked as soft actuators. Among them, various soft robotics were introduced to demonstrate the promising impact of such materials, from climbing robotic worms [32], to swimming artificial jellyfish [149] and skates [186], to drug-delivery smart pill wrap [67]. Although stimuli-responsive materials in soft actuators are recognized as the primary element for next-generation robotics, there are grand challenges facing in this field before they can be implemented in current robotic systems.

Current soft actuators heavily depend on stimuli-responsive materials with a single stimulus; therefore, the performance of actuators is limited by the materials' physiochemical properties. In order to meet complicated needs from engineering applications, the combination of multiple stimuli-responsive materials could be a direct next step to couple different environmental and engineered stimuli and achieve complex deformation and actuation capability. In such design method, each stimulus of actuators should have similar mechanical properties to avoid possible actuation disorder, which would take precise mechanics modeling.

In addition, increasing motion and energy-transfer efficiency in soft actuators is currently the most heavily invested research direction. It requires complex structural designs that span multiple scales and dimensions. This complexity poses challenges in terms of manufacturing. One key requirement for these manufacturing technologies is high precision, in order to ensure the desired functionality of soft actuators. Another important consideration is economic feasibility. High precision requirement would need manufacturing technologies like photo-lithography, which is expensive and not scalable. Therefore, high-precision manufacturing method needs to be couple in the design consideration of soft actuators in optimizing processes, minimizing material waste, and streamlining production workflows.

Another challenge is to develop non-toxic and biodegradable stimuli-responsive materials, as it is crucial for biomedical use. Traditionally, non-toxic materials are regulated to be free from heavy metals, harmful chemicals, or any components that can pose a risk to human health or the environment. For materials used in human, no toxicity is not sufficient. No allergic reactions and other adverse effects are also required to be completely avoided, particularly when these devices are implanted, used in medical procedures, or interact with living organisms. With the increasing understanding of the harm in micro-plastics [198], biodegradability is not only an important consideration for environmental impact, but also for long-term implants, which cannot or are difficult to be removed from the body. Biodegradable stimuli-responsive materials can naturally break down over time and be absorbed or eliminated by the body without leaving any harmful residues. This property is particularly important for implantable devices or those used in drug delivery systems where the actuator may need to degrade after fulfilling its intended purpose. By developing non-toxic and biodegradable stimuli-responsive materials, we can expand the application of soft actuators to broader biomedical applications.

More importantly, the durability of soft actuation materials is another issue that hinders the implementation to industrial robotic systems. Fatigue of the material affects its total actuation cycles, and therefore, it has been heavily investigated in recent years [199]. Other factors that have been paid less attention include the mechanical strength [200] and anti-fouling capability [201], which could be the next focal point to explore.

Currently, it is still rare to widely deploy and accept soft actuators in commercial robotic ecosystem. Before addressing the aforementioned challenges, researchers in the fields of materials science, computer science, biology, and mechanical engineering involved in soft robotics need to collaboratively work together and seek innovative solutions to create satisfying soft stimuli-responsive materials for soft actuators implemented in industrial robotic systems.

Acknowledgments: This work is supported by National Natural Science Foundation of China General Program (BC0201038), Science Fund Program for Excellent Young Scientists (Overseas) (BE0200017) and Shanghai Jiao Tong University "Deep Blue" Program (WH410260402/019). National Funded Postdoctoral Researcher Program of China (GZC20231584), and Hong Kong Research Grants Council (25228722).

Conflict of Interest: All authors declare that they have no competing financial interests.

References

1. Sitti, M., Miniature soft robots - road to the clinic. Nat Rev Mater 2018, 3 (6), 74-75.
2. Cianchetti, M.; Laschi, C.; Menciassi, A.; Dario, P., Biomedical applications of soft robotics. Nat Rev Mater 2018, 3 (6), 143-153.
3. Wallin, T. J.; Pikul, J.; Shepherd, R. F., 3D printing of soft robotic systems. Nat Rev Mater 2018, 3 (6), 84-100.
4. Laschi, C.; Mazzolai, B.; Cianchetti, M., Soft robotics: Technologies and systems pushing the boundaries of robot abilities. Sci Robot 2016, 1 (1).
5. Jinhao Li, J. C., Baoyang Lu & Guoying Gu, 3D-printed PEDOT: PSS for soft robotics. Nature Reviews Materials 2023, 8, 604-622.
6. Rus, D.; Tolley, M. T., Design, fabrication and control of soft robots. Nature 2015, 521 (7553), 467-475.
7. Li, M.; Pal, A.; Aghakhani, A.; Pena-Francesch, A.; Sitti, M., Soft actuators for real-world applications. Nat Rev Mater 2022, 7 (3), 235-249.
8. Shintake, J.; Cacucciolo, V.; Floreano, D.; Shea, H., Soft Robotic Grippers. Adv Mater 2018, 30 (29).

9. Zhang, Y. F.; Ng, C. J. X.; Chen, Z.; Zhang, W.; Panjwani, S.; Kowsari, K.; Yang, H. Y.; Ge, Q., Miniature Pneumatic Actuators for Soft Robots by High-Resolution Multimaterial 3D Printing. Adv Mater Technol-Us 2019, 4 (10).
10. Liu, Y. H.; Luo, K.; Wang, S.; Song, X. D.; Zhang, Z. J.; Tian, Q.; Hu, H. Y., A Soft and Bistable Gripper with Adjustable Energy Barrier for Fast Capture in Space. Soft Robot 2023, 10 (1), 77-87.
11. Mirfakhrai, T.; Madden, J. D. W.; Baughman, R. H., Polymer artificial muscles. Mater Today 2007, 10 (4), 30-38.
12. Christianson, C.; Goldberg, N. N.; Deheyn, D. D.; Cai, S. Q.; Tolley, M. T., Translucent soft robots driven by frameless fluid electrode dielectric elastomer actuators. Sci Robot 2018, 3 (17).
13. Hines, L.; Petersen, K.; Lum, G. Z.; Sitti, M., Soft Actuators for Small-Scale Robotics. Adv Mater 2017, 29 (13).
14. Feng, M.; Yang, D. Z.; Ren, L.; Wei, G. W.; Gu, G. Y., X-crossing pneumatic artificial muscles. Sci Adv 2023, 9 (38).
15. Xie, Z. X.; Yuan, F. Y.; Liu, J. Q.; Tian, L. F.; Chen, B. H.; Fu, Z. Q.; Mao, S. Z.; Jin, T. T.; Wang, Y.; He, X.; Wang, G.; Mo, Y. R.; Ding, X. L.; Zhang, Y. H.; Laschi, C.; Wen, L., Octopus-inspired sensorized soft arm for environmental interaction. Sci Robot 2023, 8 (84).
16. Van Meerbeek, I. M.; De Sa, C. M.; Shepherd, R. F., Soft optoelectronic sensory foams with proprioception. Sci Robot 2018, 3 (24).
17. Bai, H. D.; Li, S.; Barreiros, J.; Tu, Y. Q.; Pollock, C. R.; Shepherd, R. F., Stretchable distributed fiber-optic sensors. Science 2020, 370 (6518), 848-+.
18. Shih, B.; Shah, D.; Li, J. X.; Thuruthel, T. G.; Park, Y. L.; Iida, F.; Bao, Z. A.; Kramer-Bottiglio, R.; Tolley, M. T., Electronic skins and machine learning for intelligent soft robots. Sci Robot 2020, 5 (41).
19. Liu, F. Y.; Deswal, S.; Christou, A.; Sandamirskaya, Y.; Kaboli, M.; Dahiya, R., Neuro-inspired electronic skin for robots. Sci Robot 2022, 7 (67).
20. Justus, K. B.; Hellebrekers, T.; Lewis, D. D.; Wood, A.; Ingham, C.; Majidi, C.; Leduc, P. R.; Tan, C., A biosensing soft robot: Autonomous parsing of chemical signals through integrated organic and inorganic interfaces. Sci Robot 2019, 4 (31).
21. Kim, Y.; Parada, G. A.; Liu, S. D.; Zhao, X. H., Ferromagnetic soft continuum robots. Sci Robot 2019, 4 (33).
22. Son, D.; Gilbert, H.; Sitti, M., Magnetically Actuated Soft Capsule Endoscope for Fine-Needle Biopsy. Soft Robot 2020, 7 (1), 10-21.
23. Han, M. D.; Chen, L.; Aras, K.; Liang, C. M.; Chen, X. X.; Zhao, H. B.; Li, K.; Faye, N. R.; Sun, B. H.; Kim, J. H.; Bai, W. B.; Yang, Q. S.; Ma, Y. H.; Lu, W.; Song, E. M.; Baek, J. M.; Lee, Y. J.; Liu, C.; Model, J. B.; Yang, G. J.; Ghaffari, R.; Huang, Y. G.; Efimov, I. R.; Rogers, J. A., Catheter-integrated soft multilayer electronic arrays for multiplexed sensing and actuation during cardiac surgery. Nat Biomed Eng 2020, 4 (10), 997-1009.
24. Gu, G. Y. R.; Zhang, N. B.; Xu, H. P.; Lin, S. T.; Yu, Y.; Chai, G. H.; Ge, L. S.; Yang, H. L.; Shao, Q. W.; Sheng, X. J.; Zhu, X. Y.; Zhao, X. H., A soft neuroprosthetic hand providing simultaneous myoelectric control and tactile feedback. Nat Biomed Eng 2023, 7 (4), 589-598.
25. Pal, A.; Restrepo, V.; Goswami, D.; Martinez, R. V., Exploiting Mechanical Instabilities in Soft Robotics: Control, Sensing, and Actuation. Adv Mater 2021, 33 (19).
26. Ma, K. Y.; Chirarattananon, P.; Fuller, S. B.; Wood, R. J., Controlled Flight of a Biologically Inspired, Insect-Scale Robot. Science 2013, 340 (6132), 603-607.
27. Ren, Z. Y.; Hu, W. Q.; Dong, X. G.; Sitti, M., Multi-functional soft-bodied jellyfish-like swimming. Nat Commun 2019, 10.
28. Whitesides, G. M., Soft Robotics. Angew Chem Int Edit 2018, 57 (16), 4258-4273.
29. De Volder, M.; Reynaerts, D., Pneumatic and hydraulic microactuators: a review. J Micromech Microeng 2010, 20 (4).
30. Mosadegh, B.; Polygerinos, P.; Keplinger, C.; Wennstedt, S.; Shepherd, R. F.; Gupta, U.; Shim, J.; Bertoldi, K.; Walsh, C. J.; Whitesides, G. M., Pneumatic Networks for Soft Robotics that Actuate Rapidly. Adv Funct Mater 2014, 24 (15), 2163-2170.
31. Shepherd, R. F.; Ilievski, F.; Choi, W.; Morin, S. A.; Stokes, A. A.; Mazzeo, A. D.; Chen, X.; Wang, M.; Whitesides, G. M., Multigait soft robot. P Natl Acad Sci USA 2011, 108 (51), 20400-20403.
32. Gu, G. Y.; Zou, J.; Zhao, R. K.; Zhao, X. H.; Zhu, X. Y., Soft wall-climbing robots. Sci Robot 2018, 3 (25).
33. Cao, J. W.; Qin, L.; Liu, J.; Ren, Q. Y.; Foo, C. C.; Wang, H. Q.; Lee, H. P.; Zhu, J., Untethered soft robot capable of stable locomotion using soft electrostatic actuators. Extreme Mech Lett 2018, 21, 9-16.
34. Graule, M. A.; Chirarattananon, P.; Fuller, S. B.; Jafferis, N. T.; Ma, K. Y.; Spenko, M.; Kornbluh, R.; Wood, R. J., Perching and takeoff of a robotic insect on overhangs using switchable electrostatic adhesion. Science 2016, 352 (6288), 978-982.
35. Ji, X. B.; Liu, X. C.; Cacucciolo, V.; Imboden, M.; Civet, Y.; El Haitami, A.; Cantin, S.; Perriard, Y.; Shea, H., An autonomous untethered fast soft robotic insect driven by low-voltage dielectric elastomer actuators. Sci Robot 2019, 4 (37).

36. Dye, D., SHAPE MEMORY ALLOYS Towards practical actuators. Nat Mater 2015, 14 (8), 760-761.
37. Rodrigue, H.; Wang, W.; Han, M. W.; Kim, T. J. Y.; Ahn, S. H., An Overview of Shape Memory Alloy-Coupled Actuators and Robots. Soft Robot 2017, 4 (1), 3-15.
38. Seok, S.; Onal, C. D.; Cho, K. J.; Wood, R. J.; Rus, D.; Kim, S., Meshworm: A Peristaltic Soft Robot with Antagonistic Nickel Titanium Coil Actuators. Ieee-Asme T Mech 2013, 18 (5), 1485-1497.
39. Aksoy, B.; Shea, H., Reconfigurable and Latchable Shape-Morphing Dielectric Elastomers Based on Local Stiffness Modulation. Adv Funct Mater 2020, 30 (27).
40. Lima, M. D.; Li, N.; de Andrade, M. J.; Fang, S. L.; Oh, J.; Spinks, G. M.; Kozlov, M. E.; Haines, C. S.; Suh, D.; Foroughi, J.; Kim, S. J.; Chen, Y. S.; Ware, T.; Shin, M. K.; Machado, L. D.; Fonseca, A. F.; Madden, J. D. W.; Voit, W. E.; Galvao, D. S.; Baughman, R. H., Electrically, Chemically, and Photonically Powered Torsional and Tensile Actuation of Hybrid Carbon Nanotube Yarn Muscles. Science 2012, 338 (6109), 928-932.
41. Mu, J. K.; de Andrade, M. J.; Fang, S. L.; Wang, X. M.; Gao, E. L.; Li, N.; Kim, S. H.; Wang, H. Z.; Hou, C. Y.; Zhang, Q. H.; Zhu, M. F.; Qian, D.; Lu, H. B.; Kongahage, D.; Talebian, S.; Foroughi, J.; Spinks, G.; Kim, H.; Ware, T. H.; Sim, H. J.; Lee, D. Y.; Jang, Y.; Kim, S. J.; Baughman, R. H., Sheath-run artificial muscles. Science 2019, 365 (6449), 150-+.
42. Kanik, M.; Orguc, S.; Varnavides, G.; Kim, J.; Benavides, T.; Gonzalez, D.; Akintilo, T.; Tasan, C. C.; Chandrakasan, A. P.; Fink, Y.; Anikeeva, P., Strain-programmable fiber-based artificial muscle. Science 2019, 365 (6449), 145-+.
43. Yuan, J. K.; Neri, W.; Zakri, C.; Merzeau, P.; Kratz, K.; Lendlein, A.; Poulin, P., Shape memory nanocomposite fibers for untethered high-energy microengines. Science 2019, 365 (6449), 155-+.
44. Haines, C. S.; Lima, M. D.; Li, N.; Spinks, G. M.; Foroughi, J.; Madden, J. D. W.; Kim, S. H.; Fang, S. L.; de Andrade, M. J.; Göktepe, F.; Göktepe, Ö.; Mirvakili, S. M.; Naficy, S.; Lepró, X.; Oh, J. Y.; Kozlov, M. E.; Kim, S. J.; Xu, X. R.; Swedlove, B. J.; Wallace, G. G.; Baughman, R. H., Artificial Muscles from Fishing Line and Sewing Thread. Science 2014, 343 (6173), 868-872.
45. Wang, Z. B.; Wu, Y. G.; Wu, D. Z.; Sun, D. H.; Lin, L. W., Soft magnetic composites for highly deformable actuators by four-dimensional electrohydrodynamic printing. Compos Part B-Eng 2022, 231.
46. Ju, Y. W.; Hu, R.; Xie, Y.; Yao, J. P.; Li, X. X.; Lv, Y. L.; Han, X. T.; Cao, Q. L.; Li, L., Reconfigurable magnetic soft robots with multimodal locomotion. Nano Energy 2021, 87.
47. Wang, Z. B.; Xu, Z. J.; Zhu, B.; Zhang, Y.; Lin, J. W.; Wu, Y. G.; Wu, D. Z., Design, fabrication and application of magnetically actuated micro/nanorobots: a review. Nanotechnology 2022, 33 (15).
48. Wang, Z. B.; Wu, Y. G.; Zhu, B.; Chen, Q. X.; Wang, L. Y.; Zhao, Y.; Sun, D. H.; Zheng, J. Y.; Wu, D. Z., A magnetic soft robot with multimodal sensing capability by multimaterial direct ink writing. Addit Manuf 2023, 61.
49. Verra, M.; Firrincieli, A.; Chiurazzi, M.; Mariani, A.; Lo Secco, G.; Forcignanò, E.; Koulaouzidis, A.; Menciassi, A.; Dario, P.; Ciuti, G.; Arezzo, A., Robotic-Assisted Colonoscopy Platform with a Magnetically-Actuated Soft-Tethered Capsule. Cancers 2020, 12 (9).
50. Yim, S.; Sitti, M., Design and Rolling Locomotion of a Magnetically Actuated Soft Capsule Endoscope. Ieee T Robot 2012, 28 (1), 183-194.
51. Wang, X.; Yang, B. S.; Tan, D.; Li, Q.; Song, B.; Wu, Z. S.; del Campo, A.; Kappl, M.; Wang, Z. K.; Gorb, S. N.; Liu, S.; Xue, L. J., Bioinspired footed soft robot with unidirectional all-terrain mobility. Mater Today 2020, 35, 42-49.
52. Gorissen, B.; Milana, E.; Baeyens, A.; Broeders, E.; Christiaens, J.; Collin, K.; Reynaerts, D.; De Volder, M., Hardware Sequencing of Inflatable Nonlinear Actuators for Autonomous Soft Robots. Adv Mater 2019, 31 (3).
53. Li, S. G.; Vogt, D. M.; Rus, D.; Wood, R. J., Fluid-driven origami-inspired artificial muscles. P Natl Acad Sci USA 2017, 114 (50), 13132-13137.
54. Siéfert, E.; Reyssat, E.; Bico, J.; Roman, B., Bio-inspired pneumatic shape-morphing elastomers. Nat Mater 2019, 18 (1), 24-+.
55. Mutlu, R.; Alici, G.; Li, W. H., A Soft Mechatronic Microstage Mechanism Based on Electroactive Polymer Actuators. Ieee-Asme T Mech 2016, 21 (3), 1467-1478.
56. Hajiesmaili, E.; Clarke, D. R., Reconfigurable shape-morphing dielectric elastomers using spatially varying electric fields. Nat Commun 2019, 10.
57. Chortos, A.; Hajiesmaili, E.; Morales, J.; Clarke, D. R.; Lewis, J. A., 3D Printing of Interdigitated Dielectric Elastomer Actuators. Adv Funct Mater 2020, 30 (1).
58. Pelrine, R.; Kornbluh, R.; Pei, Q. B.; Joseph, J., High-speed electrically actuated elastomers with strain greater than 100%. Science 2000, 287 (5454), 836-839.
59. Duduta, M.; Hajiesmaili, E.; Zhao, H.; Wood, R. J.; Clarke, D. R., Realizing the potential of dielectric elastomer artificial muscles. P Natl Acad Sci USA 2019, 116 (7), 2476-2481.
60. Kotikian, A.; Truby, R. L.; Boley, J. W.; White, T. J.; Lewis, J. A., 3D Printing of Liquid Crystal Elastomeric Actuators with Spatially Programed Nematic Order. Adv Mater 2018, 30 (10).

61. Jin, B. J.; Song, H. J.; Jiang, R. Q.; Song, J. Z.; Zhao, Q.; Xie, T., Programming a crystalline shape memory polymer network with thermo- and photo-reversible bonds toward a single-component soft robot. Sci Adv 2018, 4 (1).
62. Chen, T.; Bilal, O. R.; Shea, K.; Daraio, C., Harnessing bistability for directional propulsion of soft, untethered robots. P Natl Acad Sci USA 2018, 115 (22), 5698-5702.
63. Kotikian, A.; McMahan, C.; Davidson, E. C.; Muhammad, J. M.; Weeks, R. D.; Daraio, C.; Lewis, J. A., Untethered soft robotic matter with passive control of shape morphing and propulsion. Sci Robot 2019, 4 (33).
64. Wang, Y. S.; Huang, W. W.; Wang, Y.; Mu, X.; Ling, S. J.; Yu, H. P.; Chen, W. S.; Guo, C. C.; Watson, M. C.; Yu, Y. J.; Black, L. D.; Li, M.; Omenetto, F. G.; Li, C. M.; Kaplan, D. L., Stimuli-responsive composite biopolymer actuators with selective spatial deformation behavior. P Natl Acad Sci USA 2020, 117 (25), 14602-14608.
65. Bai, R. and Bhattacharya, K. Photomechanical coupling in photoactive nematic elastomers. Journal of the Mechanics and Physics of Solids. 2020. 144, p.104115.
66. Kim, Y.; Zhao, X. H., Magnetic Soft Materials and Robots. Chem Rev 2022, 122 (5), 5317-5364.
67. Pena-Francesch, A., Zhang, Z., Marks, L., Cabanach, P., Richardson, K., Sheehan, D., McCracken, J., Shahsavan, H. and Sitti, M. Macromolecular radical networks for organic soft magnets. Matter. 2024
68. Lu, H. J.; Zhang, M.; Yang, Y. Y.; Huang, Q.; Fukuda, T.; Wang, Z. K.; Shen, Y. J., A bioinspired multilegged soft millirobot that functions in both dry and wet conditions. Nat Commun 2018, 9.
69. Dong, X. G.; Lum, G. Z.; Hu, W. Q.; Zhang, R. J.; Ren, Z. Y.; Onck, P. R.; Sitti, M., Bioinspired cilia arrays with programmable nonreciprocal motion and metachronal coordination. Sci Adv 2020, 6 (45).
70. Lum, G. Z.; Ye, Z.; Dong, X. G.; Marvi, H.; Erin, O.; Hu, W. Q.; Sitti, M., Shape-programmable magnetic soft matter. P Natl Acad Sci USA 2016, 113 (41), E6007-E6015.
71. Gu, H. R.; Boehler, Q.; Cui, H. Y.; Secchi, E.; Savorana, G.; De Marco, C.; Gervasoni, S.; Peyron, Q.; Huang, T. Y.; Pane, S.; Hirt, A. M.; Ahmed, D.; Nelson, B. J., Magnetic cilia carpets with programmable metachronal waves. Nat Commun 2020, 11 (1).
72. Nelson, B. J.; Kaliakatsos, I. K.; Abbott, J. J., Microrobots for Minimally Invasive Medicine. Annu Rev Biomed Eng 2010, 12, 55-85.
73. Huang, H. W.; Uslu, F. E.; Katsamba, P.; Lauga, E.; Sakar, M. S.; Nelson, B. J., Adaptive locomotion of artificial microswimmers. Sci Adv 2019, 5 (1).
74. Lee, H.; Jang, Y.; Choe, J. K.; Lee, S.; Song, H.; Lee, J. P.; Lone, N.; Kim, J., 3D-printed programmable tensegrity for soft robotics. Sci Robot 2020, 5 (45).
75. Cao, L. X.; Yu, D. H.; Xia, Z. S.; Wan, H. Y.; Liu, C. K.; Yin, T.; He, Z. Z., Ferromagnetic Liquid Metal Putty-Like Material with Transformed Shape and Reconfigurable Polarity. Adv Mater 2020, 32 (17).
76. Sitti, M. & Wiersma, D. S. Pros and cons: magnetic versus optical microrobots. Adv. Mater. 32, 1906766 (2020).
77. Liu, Y. et al. Humidity- and photo-induced mechanical actuation of cross-linked liquid crystal polymers. Adv. Mater. 29, 1604792 (2017).
78. Lancia, F., Ryabchun, A., Nguindjel, A.-D., Kwangmettatam, S. & Katsonis, N. Mechanical adaptability of artificial muscles from nanoscale molecular action. Nat. Commun. 10, 4819 (2019).
79. Shahsavan, H. et al. Bioinspired underwater locomotion of light-driven liquid crystal gels. Proc. Natl Acad. Sci. USA 117, 5125–5133 (2020).
80. Kuenstler, A. S., Kim, H. & Hayward, R. C. Liquid crystal elastomer waveguide actuators. Adv. Mater. 31, e1901216 (2019).
81. Yang, H. et al. 3D printed photoresponsive devices based on shape memory composites. Adv. Mater. 29, 1701627 (2017).
82. Liu, J. A.-C., Gillen, J. H., Mishra, S. R., Evans, B. A. & Tracy, J. B. Photothermally and magnetically controlled reconfiguration of polymer composites for soft robotics. Sci. Adv. 5, eaaw2897 (2019).
83. Wang, S. et al. Asymmetric elastoplasticity of stacked graphene assembly actualizes programmable untethered soft robotics. Nat. Commun. 11, 4359 (2020).
84. Wang, Y. et al. Light-activated shape morphing and light-tracking materials using biopolymer-based programmable photonic nanostructures. Nat. Commun. 12, 1651 (2021).
85. Cai, G., Ciou, J.-H., Liu, Y., Jiang, Y. & Lee, P. S. Leaf-inspired multiresponsive MXene-based actuator for programmable smart devices. Sci. Adv. 5, eaaw7956 (2019).
86. Li, C. et al. Fast and programmable locomotion of hydrogel-metal hybrids under light and magnetic fields. Sci. Robot. 5, eabb9822 (2020).
87. Li, C. et al. Supramolecular–covalent hybrid polymers for light-activated mechanical actuation. Nat. Mater. 19, 900–909 (2020).
88. Li, J. et al. Photothermal bimorph actuators with in-built cooler for light mills, frequency switches, and soft robots. Adv. Funct. Mater. 340, 1808995 (2019).

89. Wang, W. et al. Direct laser writing of superhydrophobic PDMS elastomers for controllable manipulation via Marangoni effect. Adv. Funct. Mater. 27, 1702946 (2017).
90. Li, M., Wang, X., Dong, B. & Sitti, M. In-air fast response and high speed jumping and rolling of a light-driven hydrogel actuator. Nat. Commun. 11, 3988 (2020).
91. Zhu, Q. L. et al. Light-steered locomotion of muscle-like hydrogel by self-coordinated shape change and friction modulation. Nat. Commun. 11, 5166 (2020).
92. Zhao, Y. et al. Soft phototactic swimmer based on self-sustained hydrogel oscillator. Sci. Robot. 4, eaax7112 (2019).
93. Li, M. et al. Flexible magnetic composites for light-controlled actuation and interfaces. Proc. Natl Acad. Sci USA 115, 8119–8124 (2018).
94. Li, M., Kim, T., Guidetti, G., Wang, Y. & Omenetto, F. G. Optomechanically actuated microcilia for locally reconfigurable surfaces. Adv. Mater. 32, 2004147 (2020).
95. D. D. Han, Y. L. Zhang, J. N. Ma, Y. Q. Liu, B. Han, H. B. Sun, Light-mediated manufacture and manipulation of actuators. Advanced Materials, 2016, 28(38): 8328-8343
96. Y. H. Chen, J. J. Yang, X. Zhang, Y. Y. Feng, H. Zeng, L. Wang, et al., Light-driven bimorph soft actuators: design, fabrication, and properties. Materials Horizons, 2021,8(3): 728-757.
97. Y. Q. Liu, Z. D. Chen, D. D. Han, J. W. Mao, J. N. Ma, Y. L. Zhang, et al., Bioinspired soft robots based on the moisture-responsive graphene oxide. Advanced Science, 2021, 8(10): 2002464.
98. H. J. Lin, S. Y. Zhang, Y. Xiao, C. J. Zhang, J. X. Zhu, J. W. C. Dunlop, et al., Organic molecule-driven polymeric actuators. Macromolecular Rapid Communications, 2019, 40(7): 1800896.
99. H. Y. Tan, S. M. Liang, X. N. Yu, X. D. Song, W. Huang, L. D. Zhang, Controllable kinematics of soft polymer actuators induced by interfacial patterning. Journal of Materials Chemistry C, 2019, 7(18): 5410-5417.
100. L. D. Zhang, P. Naumov, X. M. Du, Z. G. Hu, J. Wang, Vapomechanically responsive motion of microchannel-programmed actuators. Advanced Materials, 2017, 29(37): 1702231.
101. Y. H. Bi, X. X. Du, P. P. He, C. Y. Wang, C. Liu, W. W. Guo, Smart bilayer polyacrylamide/DNA hybrid hydrogel film actuators exhibiting programmable responsive and reversible macroscopic shape deformations. Small, 2020, 16(42):1906998.
102. O. Kim, S. J. Kim, M. J. Park, Low-voltage-driven soft actuators. Chemical Communications, 2018, 54(39): 4895-4904.
103. Y. Bar-Cohen, I. A. Anderson, Effects of Hexagonal Boron Nitride Insulating Layers on the Driving Performance of Ionic Electroactive Polymer Actuators for Light-Weight Artificial Muscles. Mechanics of Soft Materials, 2019, 1(1): DOI: 10.1007/s42558-019-0005-1.
104. H. S. Wang, J. Cho, D. S. Song, J. H. Jang, J. Y. Jho, J. H. Park, High-performance electroactive polymer actuators based on ultrathick ionic polymer-metal composites with nanodispersed metal electrodes. ACS Applied Materials & Interfaces, 2017, 9(26): 21998-22005.
105. Y. S. Yan, T. Santaniello, L. G. Bettini, C. Minnai, A. Bellacicca, R. Porotti, et al., Electroactive ionic soft actuators with monolithically integrated gold nanocomposite electrodes. Advanced Materials, 2017, 29(23): 1606109.
106. D. Yang, X. X. Kong, Y. F. Ni, Z. W. Ren, S. Y. Li, J. H. Nie, et al., Ionic polymermetal composites actuator driven by the pulse current signal of triboelectric nanogenerator. Nano Energy, 2019, 66: 104139.
107. D. Barpuzary, H. Ham, D. Park, K. Kim, M. J. Park, Smart bioinspired actuators: crawling, linear, and bending motions through a multilayer design. ACS Applied Materials & Interfaces, 2021, 13(42): 50381-50391.
108. Z. Y. Cheng, Q. M. Zhang, Field-activated electroactive polymers. Mrs Bulletin, 2008, 33(3): 183-187.
109. Y. Qiu, E. Zhang, R. Plamthottam, Q. B. Pei, Dielectric elastomer artificial muscle: materials innovations and device explorations. Accounts of Chemical Research, 2019, 52(2): 316-325.
110. Y. G. Guo, L. W. Liu, Y. J. Liu, J. S. Leng, Review of dielectric elastomer actuators and their applications in soft robots. Advanced Intelligent Systems, 2021, 3(10): 2000282.
111. W. J. Sun, B. Li, F. Zhang, C. L. Fang, Y. J. Lu, X. Gao, et al., TENG-Bot: triboelectric nanogenerator powered soft robot made of uni-directional dielectric elastomer. Nano Energy, 2021, 85: 106012.
112. J. H. Youn, S. M. Jeong, G. Hwang, H. Kim, K. Hyeon, J. Park, et al., Dielectric elastomer actuator for soft robotics applications and challenges. Applied Sciences Basel, 2020, 10(2): 640.
113. H. C. Zhao, A. M. Hussain, M. Duduta, D. M. Vogt, R. J. Wood, D. R. Clarke, Compact dielectric elastomer linear actuators. Advanced Functional Materials, 2018, 28(42):1804328.
114. L. Liu, J. S. Zhang, M. Luo, H. L. Chen, Z. C. Yang, D. C. Li, et al., A bio-inspired soft-rigid hybrid actuator made of electroactive dielectric elastomers. Applied Materials Today, 2020, 21: 100814.
115. J. He, Z. Chen, Y. Xiao, X. Cao, J. Mao, J. Zhao, et al., Intrinsically anisotropic dielectric elastomer fiber actuators. ACS Materials Letters, 2022, 4(3): 472-479.
116. A. Chortos, J. Mao, J. Mueller, E. Hajiesmaili, J. A. Lewis, D. R. Clarke, Printing reconfigurable bundles of dielectric elastomer fibers. Advanced Functional Materials, 2021, 31(22): 2010643.

117. S. Ma, Y. Zhang, Y. Liang, L. Ren, W. Tian, L. Ren, High-performance ionic-polymer metal composite: toward large-deformation fast-response artificial muscles. Advanced Functional Materials, 2019, 30(7): 1908508.
118. Cezar C A, Kennedy S M, Mehta M, et al. Biphasic ferrogels for triggered drug and cell delivery[J]. Advanced healthcare materials, 2014, 3(11): 1869-1876.
119. Zrínyi M, Barsi L, Büki A. Deformation of ferrogels induced by nonuniform magnetic fields[J]. The Journal of chemical physics, 1996, 104(21): 8750-8756.
120. Haider H, Yang C H, Zheng W J, et al. Exceptionally tough and notch-insensitive magnetic hydrogels[J]. Soft Matter, 2015, 11(42): 8253-8261.
121. Schmauch M M, Mishra S R, Evans B A, et al. Chained iron microparticles for directionally controlled actuation of soft robots[J]. ACS applied materials & interfaces, 2017, 9(13): 11895-11901.
122. Kim J, Chung S E, Choi S E, et al. Programming magnetic anisotropy in polymeric microactuators[J]. Nature materials, 2011, 10(10): 747-752.
123. Erb R M, Martin J J, Soheilian R, et al. Actuating soft matter with magnetic torque[J]. Advanced Functional Materials, 2016, 26(22): 3859-3880.
124. Roeder L, Bender P, Tschöpe A, et al. Shear modulus determination in model hydrogels by means of elongated magnetic nanoprobes[J]. Journal of Polymer Science Part B: Polymer Physics, 2012, 50(24): 1772-1781.
125. Lisjak D, Mertelj A. Anisotropic magnetic nanoparticles: A review of their properties, syntheses and potential applications[J]. Progress in Materials Science, 2018, 95: 286-328.
126. Seifert J, Roitsch S, Schmidt A M. Covalent Hybrid Elastomers Based on Anisotropic Magnetic Nanoparticles and Elastic Polymers[J]. ACS Applied Polymer Materials, 2021, 3(3): 1324-1337.
127. Yu Huang, Birgitt Boschitsch Stogin, Nan Sun, Jing Wang, Shikuan Yang, and Tak-Sing Wong. A Switchable Cross-Species Liquid-Repellent Surface. Advanced Materials, vol. 29, 1604641 (2017).
128. Bowen L, Springsteen K, Feldstein H, et al. Development and validation of a dynamic model of magneto-active elastomer actuation of the origami waterbomb base[J]. Journal of Mechanisms and Robotics, 2015, 7(1): 011010.
129. Crivaro A, Sheridan R, Frecker M, et al. Bistable compliant mechanism using magneto active elastomer actuation[J]. Journal of Intelligent Material Systems and Structures, 2016, 27(15): 2049-2061.
130. Kim, Y., Yuk, H., Zhao, R. et al. Printing ferromagnetic domains for untethered fast-transforming soft materials. Nature 558, 274–279 (2018).
131. Ma et al. Magnetic Multimaterial Printing for Multimodal Shape Transformation with Tunable Properties and Shiftable Mechanical Behaviors. ACS Appl. Mater. Interfaces 2021, 13, 11, 12639–12648.
132. H. Wu, O. Wang, Y. Tian, et al. Selective Laser Sintering-Based 4D Printing of Magnetism-Responsive Grippers[J]. ACS Applied Materials & Interfaces. 2021, 13, 11, 12679-12688.
133. Shcherbakov V P, Winklhofer M. Bending of magnetic filaments under a magnetic field[J]. Physical Review E, 2004, 70(6): 061803.
134. Dzhezherya Y I, Xu W, Cherepov S V, et al. Magnetoactive elastomer based on superparamagnetic nanoparticles with Curie point close to room temperature[J]. Materials & Design, 2021, 197: 109281.
135. Fahrni F, Prins M W J, Van IJzendoorn L J. Magnetization and actuation of polymeric microstructures with magnetic nanoparticles for application in microfluidics. Journal of Magnetism and Magnetic Materials, 2009, 321(12): 1843-1850.
136. Evans B A, Fiser B L, Prins W J, et al. A highly tunable silicone-based magnetic elastomer with nanoscale homogeneity. Journal of magnetism and magnetic materials, 2012, 324(4): 501-507.
137. Cui J, Huang T Y, Luo Z, et al. Nanomagnetic encoding of shape-morphing micromachines. Nature, 2019, 575(7781): 164-168.
138. Alfadhel A, Kosel J. Magnetic nanocomposite cilia tactile sensor[J]. Advanced Materials, 2015, 27: 7888–7892.
139. Zhang J, Ren Z, Hu W, et al. Voxelated three-dimensional miniature magnetic soft machines via multimaterial heterogeneous assembly[J]. Science robotics, 2021, 6(53): eabf0112.
140. Kennedy S, Roco C, Déléris A, et al. Improved magnetic regulation of delivery profiles from ferrogels. Biomaterials, 2018, 161: 179-189.
141. X. X. Le, W. Lu, J. W. Zhang, T. Chen, Recent progress in biomimetic anisotropic hydrogel actuators. Advanced Science, 2019, 6(5): 1801584.
142. S. L. Xiang, Y. X. Su, H. Yin, C. Li, M. Q. Zhu, Visible-light-driven isotropic hydrogels as anisotropic underwater actuators. Nano Energy, 2021, 85: 105965.
143. Tang JD; Yin QF; Qiao YC; Wang TJ, Shape Morphing of Hydrogels in Alternating Magnetic Field, ACS Applied Materials& Interfaces, 2019, 11, 21194−21200.
144. Yang Gao, Xiuyuan Han, Jiaojiao Chen, Yudong Pan, Meng Yang, Linhe Lu, Jian Yang, Zhigang Suo, Tongqing Lu. Hydrogel–mesh composite for wound closure. Proceedings of the National Academy of Sciences of the United States of America. 118 e2103457118 (2021).

145. Yang H; Ji MK; Yang M; Shi MXZ; Pan YD; Zhou YF; Qi HJ; Suo ZG; Tang JD, Fabricating hydrogels to mimic biological tissues of complex shapes and high fatigue resistance, Matter, 2021, 4, 1935-1946.
146. Yifan Zhou, Xuhui Zhang, Meng Yang, Yudong Pan, Zhenjiang Du, Jose Blanchet, Zhigang Suo, Tongqing Lu. High-throughput experiments for rare-event rupture of materials. Matter. 5(2), 654 (2022).
147. X. He, S. Wang, J. Zhou, D. Zhang, Y. Xue, X. Yang, et al., Versatile and simple strategy for preparing bilayer hydrogels with Janus characteristics. ACS Applied Materials & Interfaces, 2022, 14(3): 4579-4587.
148. Xiaoshi Qian, et al. Artificial Phototropism for Omnidirectional Tracking and Harvesting of Light. Nature Nanotechnology, 14, 1048 (2019).
149. Hou, G. D.; Zhang, X.; Du, F. H.; Wu, Y. D.; Zhang, X.; et al. Self-regulated underwater phototaxis of a photoresponsive hydrogel-based phototactic vehicle. Nat Nanotechnol 2023.
150. P. Chen, Q. Ruan, R. Nasseri, et al., Light-Fueled Hydrogel Actuators with Controlled Deformation and Photocatalytic Activity. Adv. Sci. 2022,9, 2204730.
151. C. Y. Zhu, Y. Lu, L. X. Jiang, Y. L. Yu, Liquid crystal soft actuators and robots toward mixed reality. Advanced Functional Materials, 2021, 31(39): 2009835.
152. Ruobing Bai, Ying Shi Teh, Kaushik Bhattacharya, Collective behavior in the kinetics and equilibrium of solid-state photoreaction, Extreme Mechanics Letters, 2021, 43, 101160.
153. Ruobing Bai, Kaushik Bhattacharya, Photomechanical coupling in photoactive nematic elastomers, Journal of the Mechanics and Physics of Solids. 2020. https://doi.org/10.1016/j.jmps.2020.104115.
154. M. Cheng, H. Zeng, Y. F. Li, J. X. Liu, D. Luo, A. Priimagi, et al., Light-fueled polymer film capable of directional crawling, friction-controlled climbing, and self-sustained motion on a human hair. Advanced Science, 2022, 9(1): 2103090.
155. Z. Q. Shen, F. F. Chen, X. Y. Zhu, K. T. Yong, G. Y. Gu, Stimuli-responsive functional materials for soft robotics. Journal of Materials Chemistry B, 2020, 8(39): 8972-8991.
156. X. L. Pang, J. A. Lv, C. Y. Zhu, L. Qi, Y. L. Yu, Photodeformable azobenzenecontaining liquid crystal polymers and soft actuators. Advanced Materials, 2019,31(52): 1904224.
157. L. Chen, H. K. Bisoyi, Y. L. Huang, S. Huang, M. Wang, H. Yang, et al., Healable and rearrangeable networks of liquid crystal elastomers enabled by diselenide bonds. Angewandte Chemie-International Edition, 2021, 60(30): 16394-16398.
158. S. Li, H. D. Bai, Z. Liu, X. Y. Zhang, C. Q. Huang, E. N. R. Wiesner, et al., Digital light processing of liquid crystal elastomers for self-sensing artificial muscles. Science Advances, 2021, 7(30): eabg3677.
159. P. F. Lv, X. Yang, H. K. Bisoyi, H. Zeng, X. Zhang, Y. H. Chen, et al., Stimulus-driven liquid metal and liquid crystal network actuators for programmable soft robotics. Materials Horizons, 2021, 8(9): 2475-2484.
160. Z. C. Jiang, Y. Y. Xiao, X. Tong, Y. Zhao, Selective decrosslinking in liquid crystal polymer actuators for optical reconfiguration of origami and light-fueled locomotion. Angewandte Chemie-International Edition, 2019, 58(16): 5332-5337.
161. R. C. P. Verpaalen, M. P. da Cunha, T. A. P. Engels, M. G. Debije, A. P. H. J. Schenning, Liquid crystal networks on thermoplastics: reprogrammable photo-responsive actuators. Angewandte Chemie-International Edition, 2020, 59(11): 4532-4536.
162. Q. G. He, Z. J. Wang, Y. Wang, Z. J. Wang, C. H. Li, R. Annapooranan, et al., Electrospun liquid crystal elastomer microfiber actuator. Science Robotics, 2021, 6(57): 9704.
163. K. Kim, Y. H. Guo, J. Bae, S. Choi, H. Y. Song, S. Park, et al., 4D printing of hygroscopic liquid crystal elastomer actuators. Small, 2021, 17(23): 2100910.
164. Z. C. Jiang, Y. Y. Xiao, R. D. Cheng, J. B. Hou, Y. Zhao, Dynamic liquid crystalline networks for twisted fiber and spring actuators capable of fast light-driven movement with enhanced environment adaptability. Chemistry of Materials, 2021, 33(16): 6541-6552.
165. C. Song, Y. Zhang, J. Bao, et al. Photo-responsive Programmable Shape-Memory Soft Actuator Based on Liquid Crystalline Polymer/Polyurethane Network. Adv. Funct. Mater. 2023, 33, 2213771.
166. Ke Zheng, Enlai Gao, Bin Tian, Jing Liang, Qun Liu, Enbo Xue, Qian Shao, Wei Wu. Modularized Paper Actuator Based on Shape Memory Alloy, Printed Heater, and Origami. Adv. Intell. Syst. 2022,4, 2200194.
167. L. Hyun-Taek, F. Seichepine, G. Yang. Microtentacle Actuators Based on Shape Memory Alloy Smart Soft Composite. Advanced Functional Materials, 2020, 30, 2002510.
168. Xianrong Liang, Chenggang Yuan, Chaoying Wan, Xiaolong Gao, Chris Bowen, Min Pan. Soft Self-Healing Robot Driven by New Micro Two-Way Shape Memory Alloy Spring. Adv. Sci. 2024,11, 2305163.
169. Tian-Yue Wu, Qian-Yi Fang, Zhu-Long Xu, Xin-Jin Li, Wen-Xuan Ma, Ming-Shuai Chu, Jae Hyuk Lim, Kuo-Chih Chuang. Knitting Shape-Memory Alloy Wires for Riding a Robot: Constraint Matters for the Curvilinear Actuation. Adv. Intell. Syst. 2022,4, 2200035.
170. M. C. Mulakkal, R. S. Trask, V. P. Ting, A. M. Seddon, Responsive cellulose-hydrogel composite ink for 4D printing. Materials & Design, 2018, 160: 108-118.
171. Y. R. Wang, P. P. Feng, R. Liu, B. T. Song, Rational design of a porous nanofibrous actuator with highly sensitive, ultrafast, and large deformation driven by humidity. Sensors and Actuators B: Chemical, 2021, 330: 129236.

172. J. Wei, S. Jia, J. Wei, C. Ma, Z. Q. Shao, Tough and multifunctional composite film actuators based on cellulose nanofibers toward smart wearables. ACS Applied Materials & Interfaces, 2021, 13(32): 38700-38711.
173. Y. Y. Gao, Y. L. Zhang, B. Han, L. Zhu, B. Dong, H. B. Sun, Gradient assembly of polymer nanospheres and graphene oxide sheets for dual-responsive soft actuators. ACS Applied Materials & Interfaces, 2019, 11(40): 37130-37138.
174. B. Huang, G. Zhu, S. Z. Wang, Q. Y. Li, J. Viguie, H. He, et al., A gradient poly(vinyl alcohol)/polysaccharides composite film towards robust and fast stimuli-responsive actuators by interface co-precipitation. Journal of Materials Chemistry A, 2021, 9(40): 22973-22981.
175. Y. F. Zheng, H. Huang, Y. Wang, J. Zhu, J. R. Yu, Z. M. Hu, Poly (vinyl alcohol) based gradient cross-linked and reprogrammable humidity-responsive actuators. Sensors and Actuators B: Chemical, 2021, 349: 130735.
176. Y. H. Ge, R. Cao, S. J. Ye, Z. Chen, Z. F. Zhu, Y. F. Tu, et al., A bio-inspired homogeneous graphene oxide actuator driven by moisture gradients. Chemical Communications, 2018, 54(25): 3126-3129.
177. J. N. Ma, Y. L. Zhang, D. D. Han, J. W. Mao, Z. D. Chen, H. B. Sun, Programmable deformation of patterned bimorph actuator swarm. National Science Review, 2020, 7(4): 775-785.
178. B. Han, Y. Y. Gao, Y. L. Zhang, Y. Q. Liu, Z. C. Ma, Q. Guo, et al., Multi-field-coupling energy conversion for flexible manipulation of graphene-based soft robots. Nano Energy, 2020, 71: 104578.
179. Y. Y. Qiu, M. T. Wang, W. Z. Zhang, Y. X. Liu, Y. V. Li, K. Pan, An asymmetric graphene oxide film for developing moisture actuators. Nanoscale, 2018, 10(29):14060-14066.
180. J. E. Yim, S. H. Lee, S. Jeong, K. A. I. Zhang, J. Byun, Controllable porous membrane actuator by gradient infiltration of conducting polymers. Journal of Materials Chemistry A, 2021, 9(8): 5007-5015.
181. P. Wang, G. Zheng, K. Dai, C. Liu, C. Shen, Programmable micropatterned surface for single-layer homogeneous-polymer Janus actuator. Chemical Engineering Journal, 2022, 430: 133052.
182. L. Hu, Q. Zhang, X. Li, M. J. Serpe, Stimuli-responsive polymers for sensing and actuation. Materials Horizons, 2019, 6(9): 1774-1793.
183. L. Hu, Y. Wan, Q. Zhang, M. J. Serpe, Harnessing the power of stimuli-responsive polymers for actuation. Advanced Functional Materials, 2020, 30(2): 1903471.
184. K. Cho, D. Kang, H. Lee, W. G. Koh, Multi-stimuli responsive and reversible soft actuator engineered by layered fibrous matrix and hydrogel micropatterns. Chemical Engineering Journal, 2022, 427: 130879.
185. Wang, D., Zhao, B., Li, X. et al. Dexterous electrical-driven soft robots with reconfigurable chiral-lattice foot design. Nat. Commun. 14, 5067 (2023).
186. Li, G., Chen, X., Zhou, F. et al. Self-powered soft robot in the Mariana Trench. Nature 591, 66–71 (2021).
187. Henan Song, Xiaobiao Shan, Ruirui Li, Chengwei Hou. Review on the Vibration Suppression of Cantilever Beam through Piezoelectric Materials. Adv. Eng. Mater. 2022, 24, 2200408.
188. Xiangyu Gao, Jikun Yang, Jingen Wu, Xudong Xin, Zhanmiao Li, Xiaoting Yuan, Xinyi Shen, Shuxiang Dong. Piezoelectric Actuators and Motors: Materials, Designs, and Applications. Adv. Mater. Technol. 2020, 5, 1900716.
189. Dengfeng Li, Jian Li, Pengcheng Wu, Guangyao Zhao, Qing'ao Qu, and Xinge Yu. Recent Advances in Electrically Driven Soft Actuators across Dimensional Scales from 2D to 3D. Adv. Intell. Syst. 2023, 2300070.
190. Junwen Zhong, Yuan Ma, Yu Song, Qize Zhong, Yao Chu, Ilbey Karakurt, David B. Bogy, and Liwei Lin. A Flexible Piezoelectret Actuator/Sensor Patch for Mechanical Human–Machine Interfaces. ACS Nano 2019, 13, 6, 7107–7116.
191. S. Sharafkhani, M. Kokabi, High performance flexible actuator: PVDF nanofibers incorporated with axially aligned carbon nanotubes. Composites, Part B 2021, 222, 109060.
192. A. Kumar, A. Varghese, A. Sharma, M. Prasad, V. Janyani, R. P. Yadav, K. Elgaid. Recent development and futuristic applications of MEMS based piezoelectric microphones. Sens. Actuators, A 2022, 347, 113887.
193. S. Mishra, L. Unnikrishnan, S. K. Nayak, S. Mohanty, Advances in Piezoelectric Polymer Composites for Energy Harvesting Applications: A Systematic Review. Macromol. Mater. Eng. 2019, 304, 1800463.
194. A. Fath, T. Xia, W. Li, Recent Advances in the Application of Piezoelectric Materials in Microrobotic Systems. Micromachines 2022, 13, 1422.
195. D. Kim, S. A. Han, J. H. Kim, J. H. Lee, S. W. Kim, S. W. Lee, Biomolecular Piezoelectric Materials: From Amino Acids to Living Tissues. Adv. Mater. 2020, 32, 1906989.
196. Y. Wu, J. K. Yim, J. Liang, Z. Shao, M. Qi, J. Zhong, Z. Luo, X. Yan, M. Zhang, X. Wang, R. S. Fearing, R. J. Full, L. Lin, Insect-scale fast moving and ultrarobust soft robot. Sci. Rob. 2019, 4, eaax1594.
197. J. Liang, Y. Wu, J. K. Yim, H. Chen, Z. Miao, H. Liu, Y. Liu, Y. Liu, D. Wang, W. Qiu, Z. Shao, M. Zhang, X. Wang, J. Zhong, L. Lin, Electrostatic footpads enable agile insect-scale soft robots with trajectory control. Sci. Rob. 2021, 6, eabe7906.
198. Coates, G. W., & Getzler, Y. D. Chemical recycling to monomer for an ideal, circular polymer economy. Nature Reviews Materials. 2020, 5(7), 501-516.
199. Bai, R., Yang, J. and Suo, Z. Fatigue of hydrogels. European Journal of Mechanics-A/Solids. 2019. 74, pp.337-370.

200. Wang, J., Wu, B., Dhyani, A., Repetto, T., Gayle, A.J., Cho, T.H., Dasgupta, N.P. and Tuteja, A. Durable Liquid-and Solid-Repellent Elastomeric Coatings Infused with Partially Crosslinked Lubricants. ACS Applied Materials & Interfaces. 2022. 14(19), pp.22466-22475.
201. Wang, J., Wang, L., Sun, N., Tierney, R., Li, H., Corsetti, M., Williams, L., Wong, P.K. and Wong, T.S. Viscoelastic solid-repellent coatings for extreme water saving and global sanitation. Nature Sustainability. 2019 2(12), pp.1097-1105.